Measurement of the N→Δ Transition Form Factors

Hamza Atac
Temple University

Supported by the US DOE / NP award DE-SC0016577

Jefferson Lab

U.S. DEPARTMENT OF ENERGY

The N-Δ transition

Proton (938 MeV)

Delta (1232 MeV)

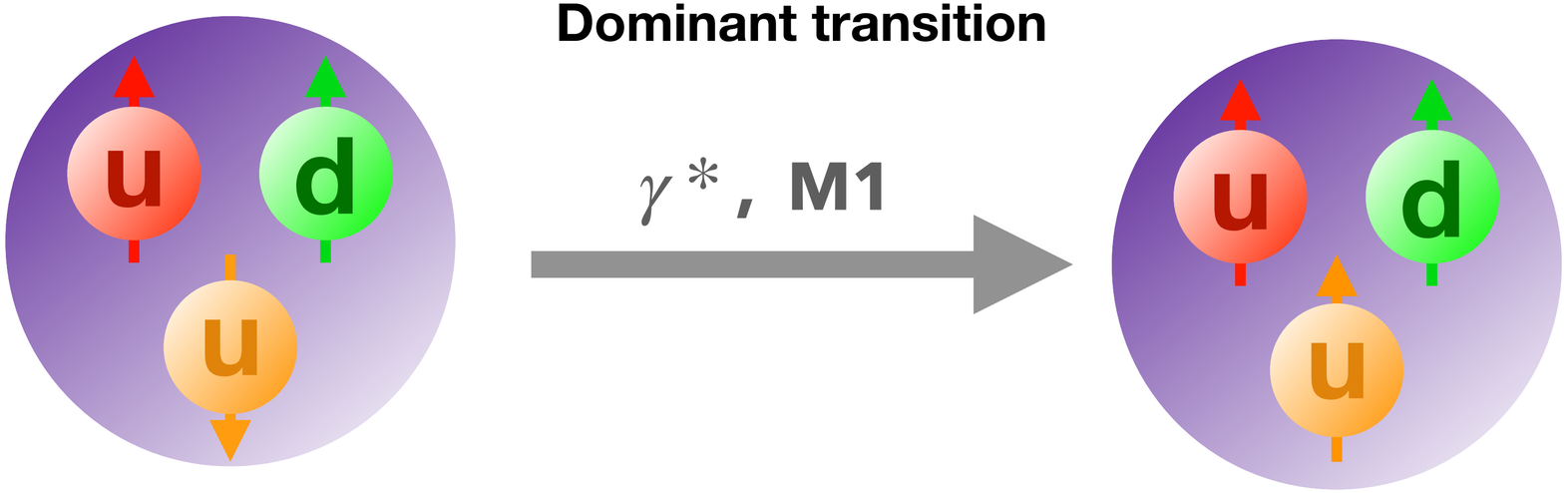

The first excited state of the proton, the Delta, can be reached through a magnetic spin flip of one of the quarks (M1).
(spherical S-wave proton WF -> spherical S-wave Delta WF)

The N-Δ transition

Proton (938 MeV) **Delta (1232 MeV)**

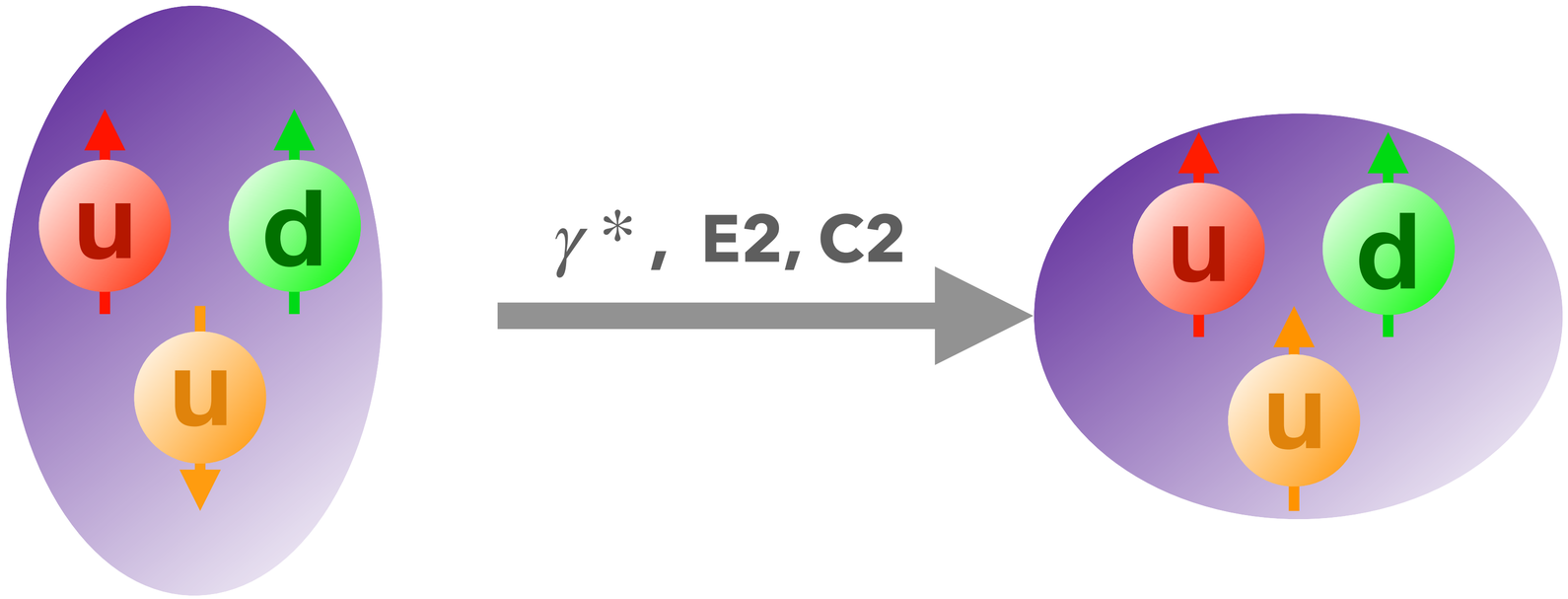

It can also be reached through a quadrupole (E2 or C2) transition from proton to delta. (The quadrupole amplitudes are associated with the existence of non-spherical components in the proton and Delta WF)

The N-Δ transition

Proton (938 MeV)

Delta (1232 MeV)

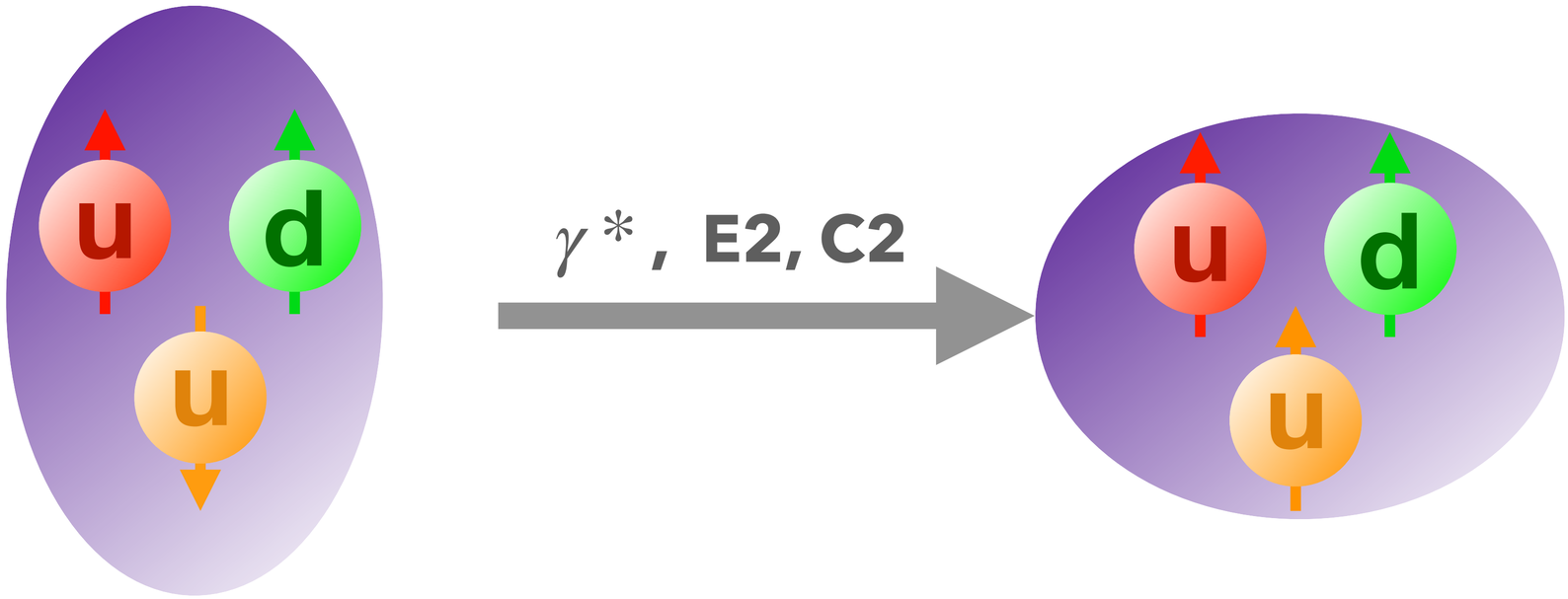

It can also be reached through a quadrupole (E2 or C2) transition from proton to delta. (The quadrupole amplitudes are associated with the existence of non-spherical components in the proton and Delta WF)

The quadrupole to dipole ratio (E2/M1 or C2/M1) is non-zero... Why?

Electric-Quadrupole to **M**agnetic-Dipole **R**atio = **EMR** = E2/M1

Coulomb-Quadrupole to **M**agnetic-Dipole **R**atio = **CMR** = C2/M1

The N-Δ transition

Proton (938 MeV)

Delta (1232 MeV)

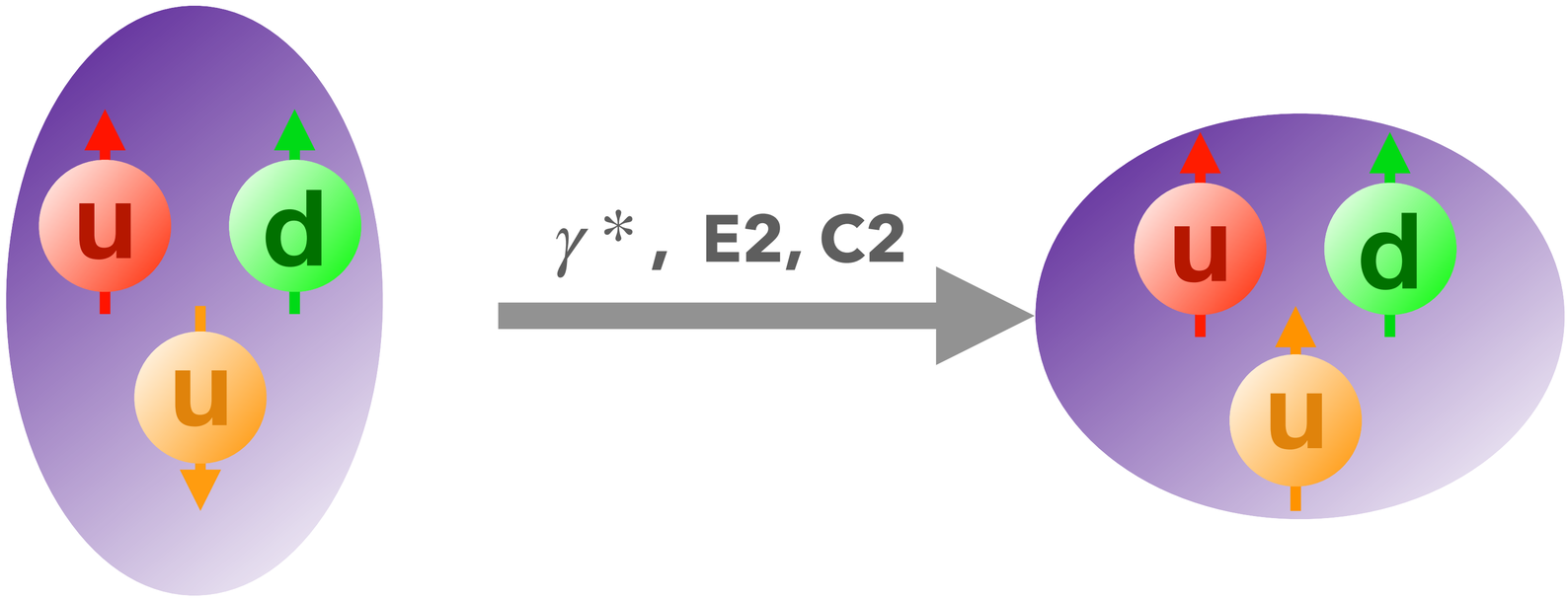

It can also be reached through a quadrupole (E2 or C2) transition from proton to delta. (The quadrupole amplitudes are associated with the existence of non-spherical components in the proton and Delta WF)

The quadrupole to dipole ratio (E2/M1 or C2/M1) is non-zero... Why?

Non-central (tensor) interactions between quarks can account for some of the spherical deviation, but not all...

The N-Δ transition

Proton (938 MeV)

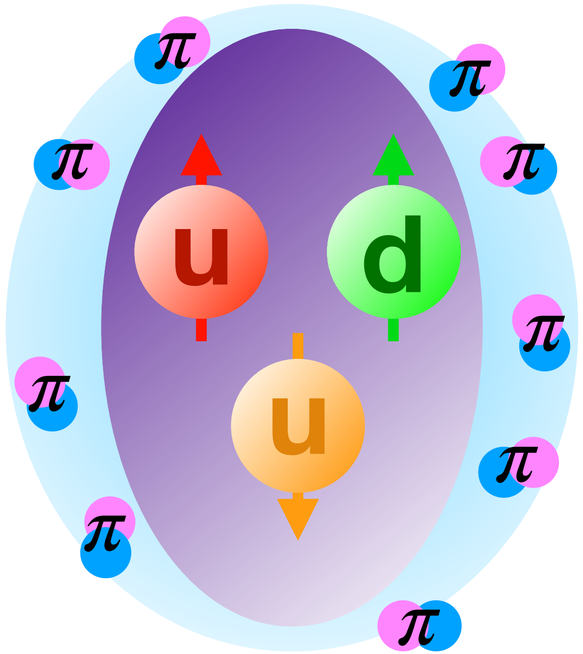

γ^*, E2, C2

Delta (1232 MeV)

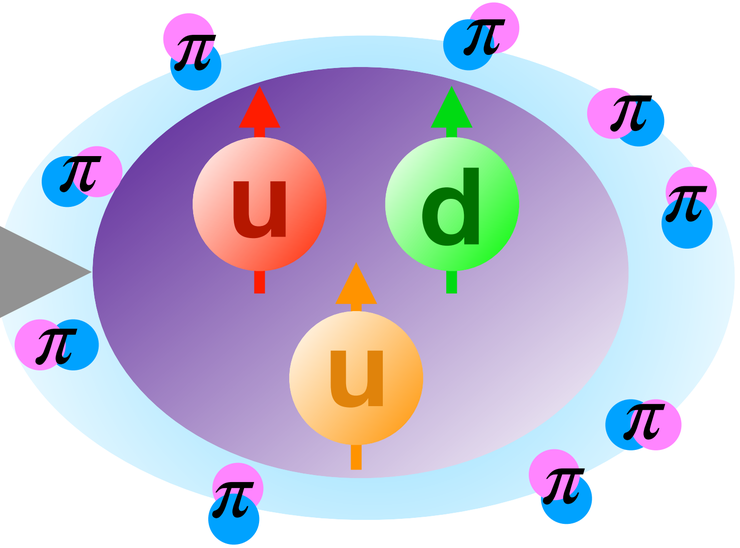

It can also be reached through a quadrupole (E2 or C2) transition from proton to delta. (The quadrupole amplitudes are associated with the existence of non-spherical components in the proton and Delta WF)

The quadrupole to dipole ratio (E2/M1 or C2/M1) is non-zero... Why?

The dynamics of a meson cloud are important to describe the structure of the nucleon.

Experimental Methodology

$$\sigma = \mathrm{J}_\Omega \, \Gamma_v \, \frac{p_{\mathrm{cm}}}{k_{\mathrm{cm}}} \left(R_T + \epsilon_L R_L + \epsilon \, R_{TT} \cos 2\phi_{X\gamma} - v_{LT} R_{LT} \cos \phi_{X\gamma} \right)$$

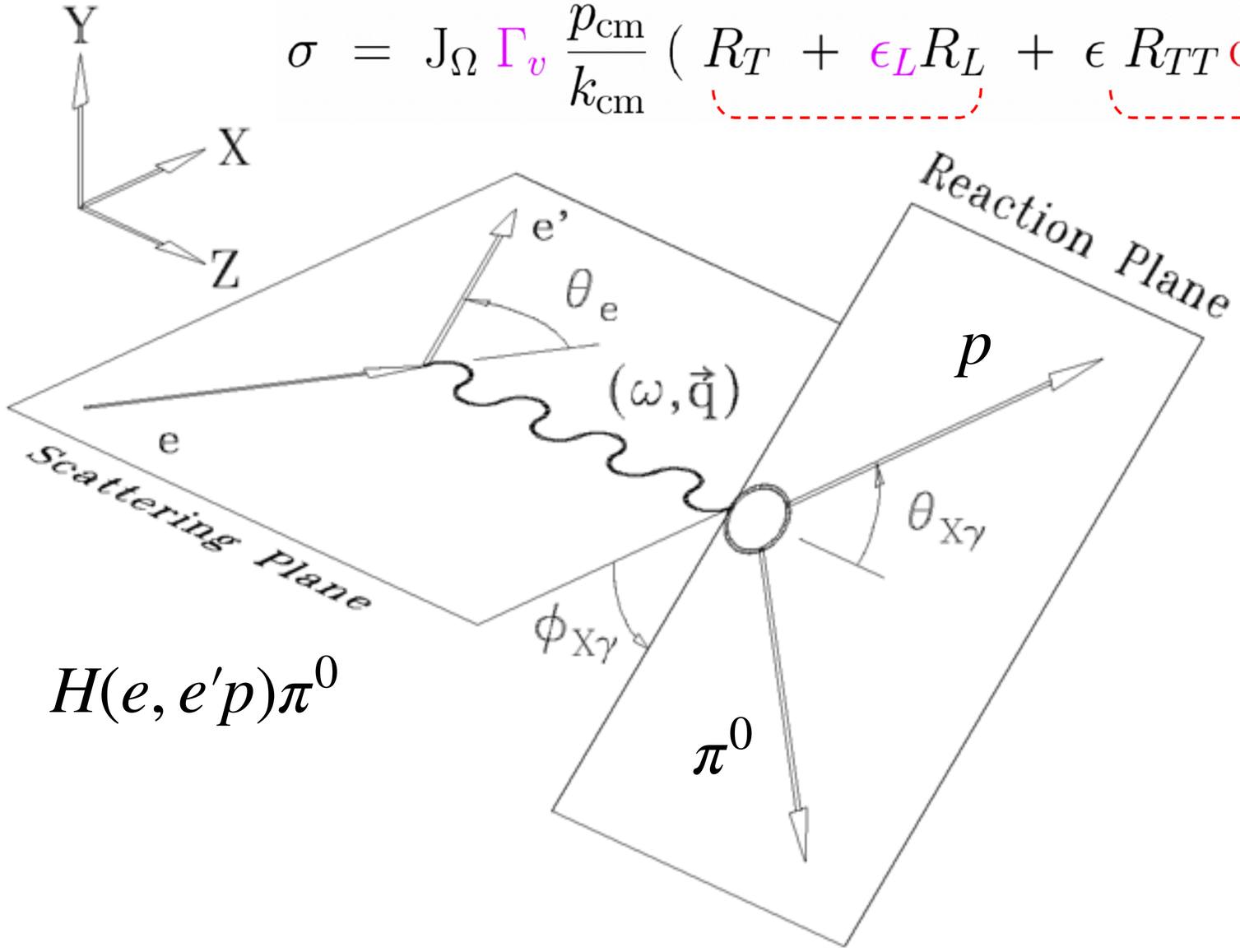

$H(e, e'p)\pi^0$

R_{TT} → **sensitive to the EMR**

R_{LT} → **sensitive to the CMR**

$R_T + R_L$ → **sensitive to $M1$**

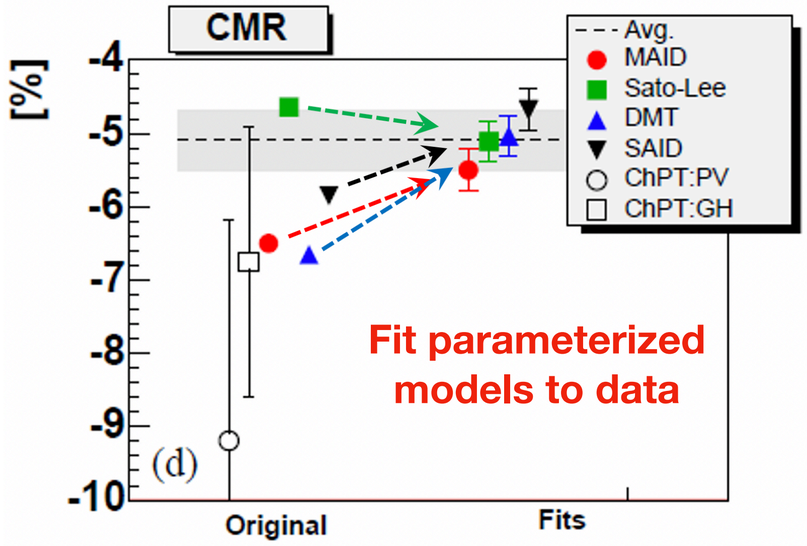

World data and status of TFFs

CMR & EMR predicted to converge at a small finite value as $Q^2 \to 0$

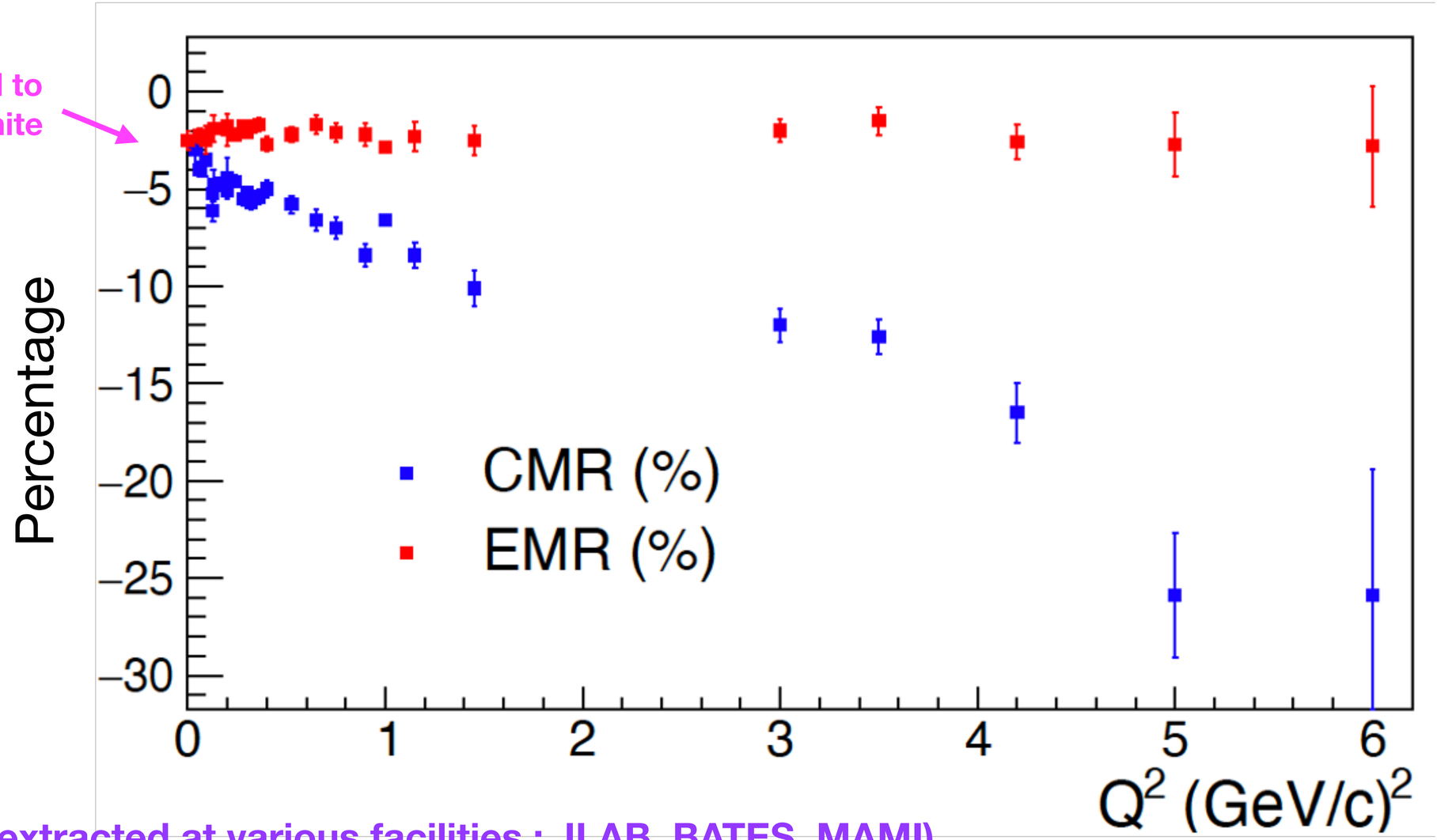

TFFs has been extracted at various facilities : JLAB, BATES, MAMI)

At large Q^2, no direct indication of EMR → 100% and CMR → constant (predicted in pQCD regime)

Lattice Calculations

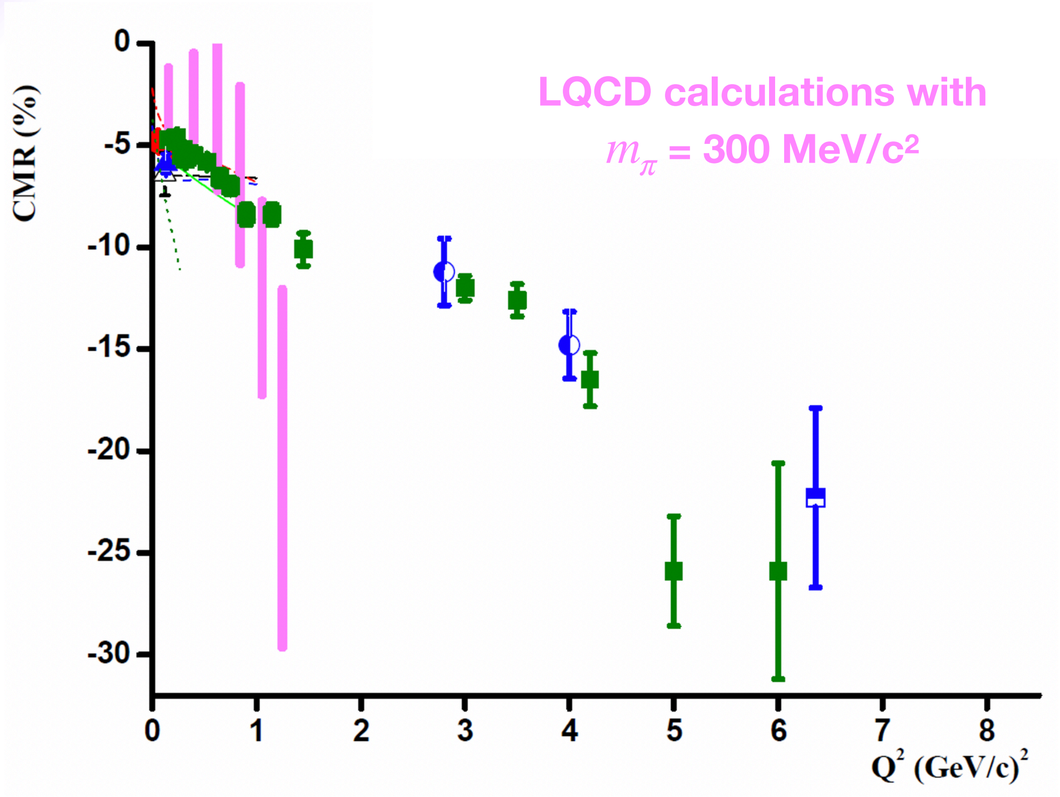

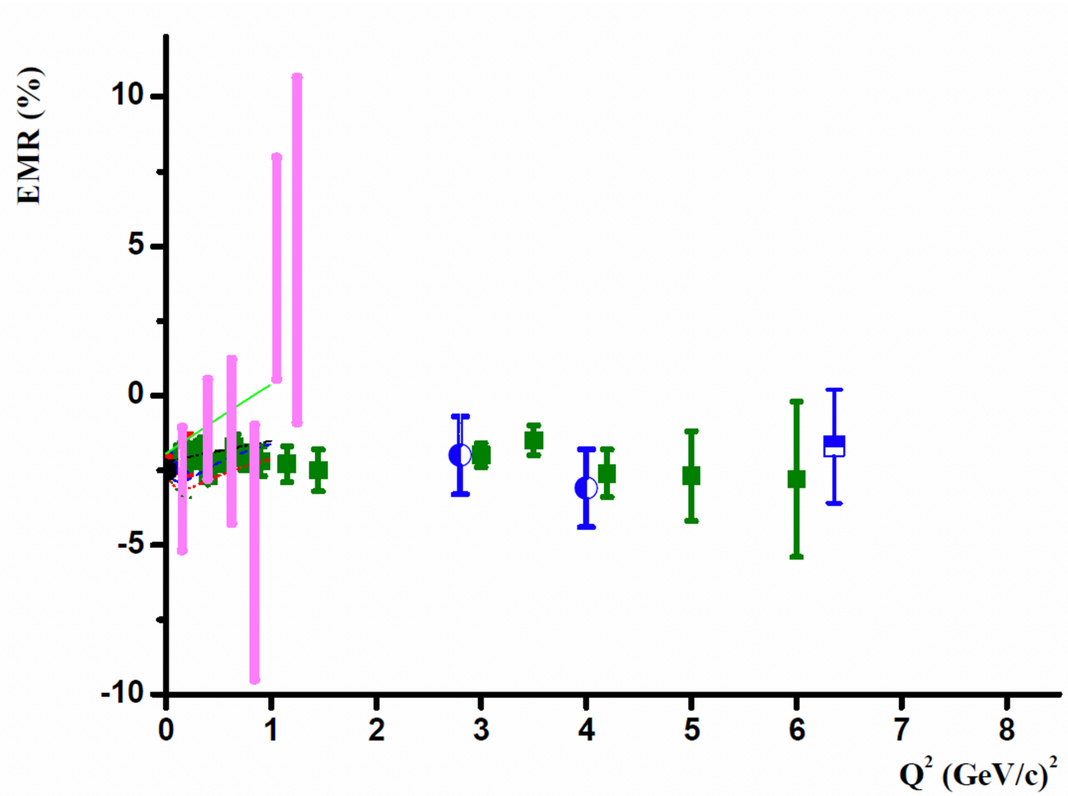

- Updated LQCD calculations are in progress → new calculations will have a physical pion mass and uncertainties comparable to experiment.
- Low Q^2 data will provide a precision benchmark for LQCD calculations.

Low Q^2 N-Δ transition form factors

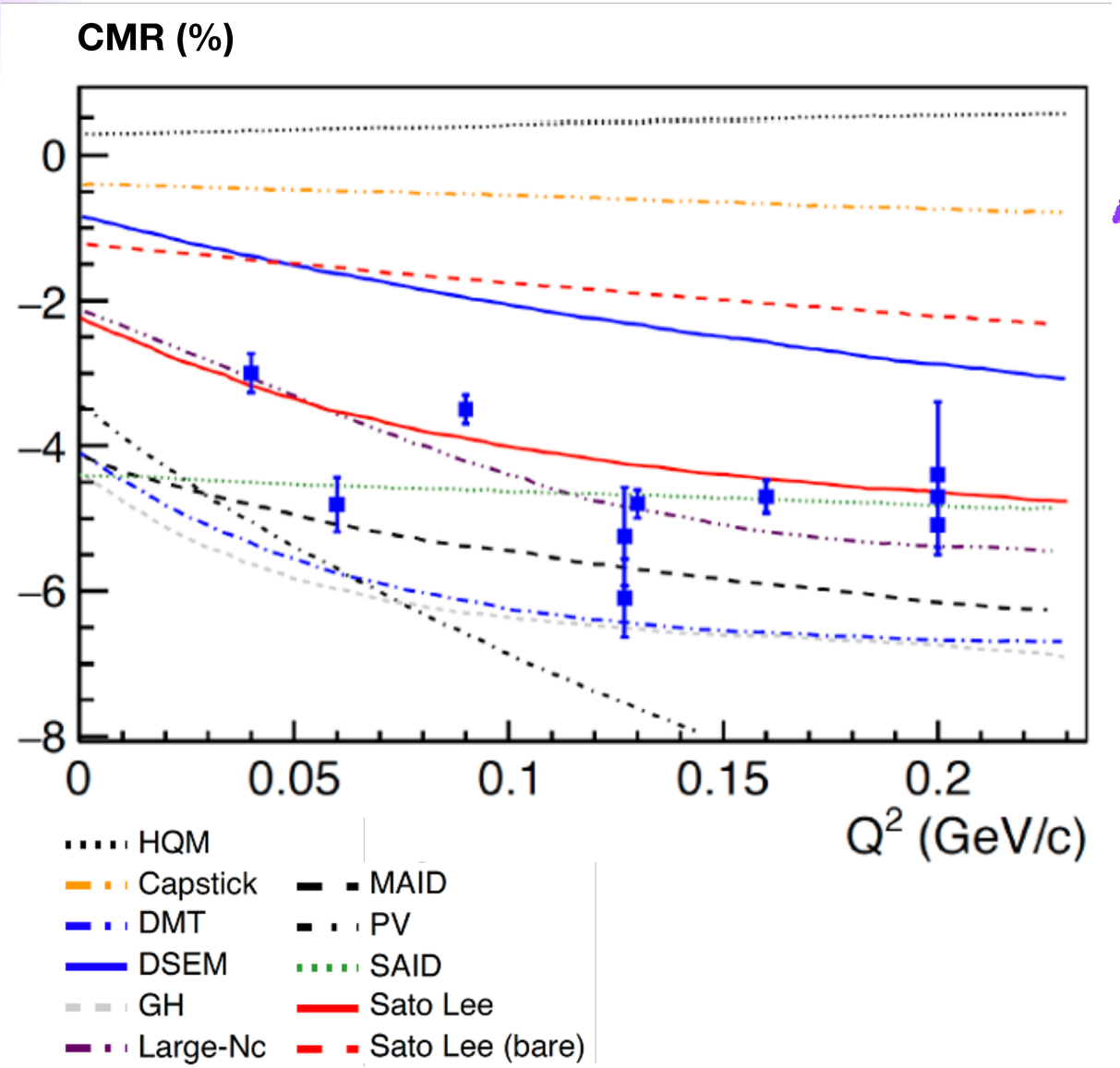

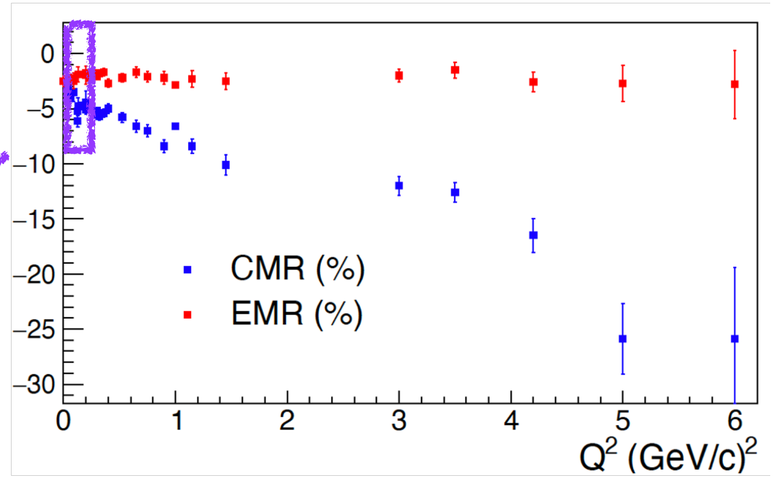

- **Low Q^2 landscape is an important region to measure:**
  - Mesonic cloud effects are predicted to be:
    - changing most rapidly over all Q^2
  - Provides an excellent test bed for ChEFT and LQCD calculations
  - Tests the predicted convergence of EMR and CMR as $Q^2 \rightarrow 0$.
  - Sparsely measured region.

Low Q^2 N-Δ transition form factors

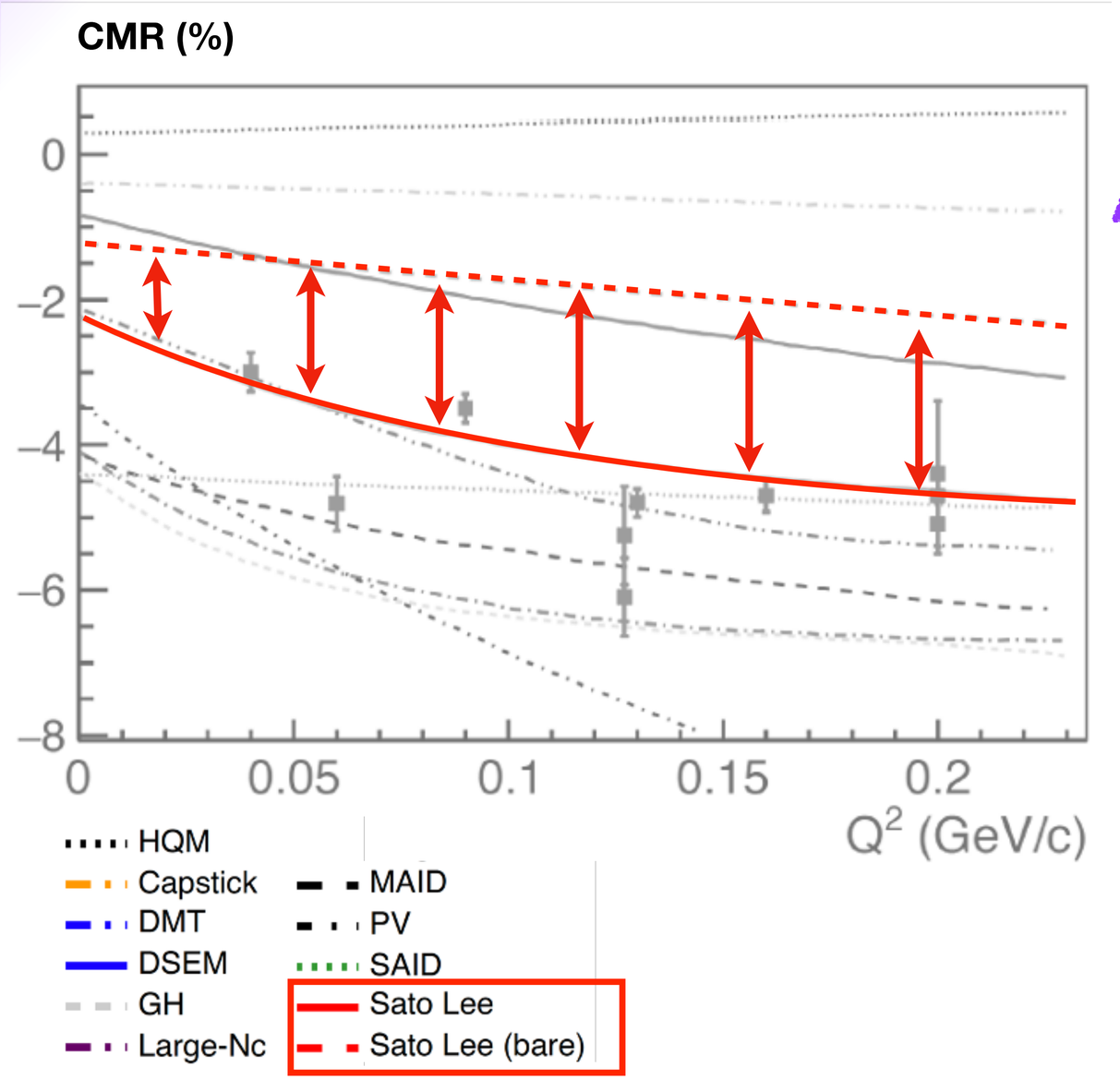

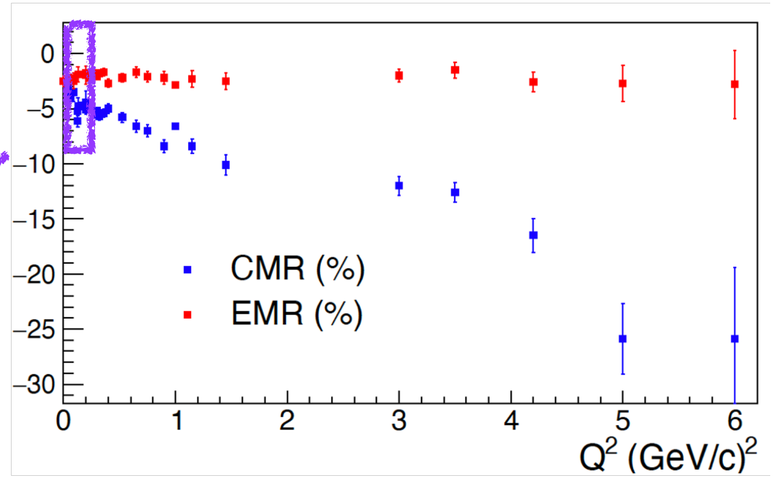

- **Low Q^2 landscape is an important region to measure:**
  - **Mesonic cloud effects** are predicted to be:
    - changing most rapidly over all Q^2
  - Provides an excellent test bed for ChEFT and LQCD calculations
  - Tests the predicted convergence of EMR and CMR as $Q^2 \rightarrow 0$.
  - Sparsely measured region.

Low Q^2 N-Δ transition form factors

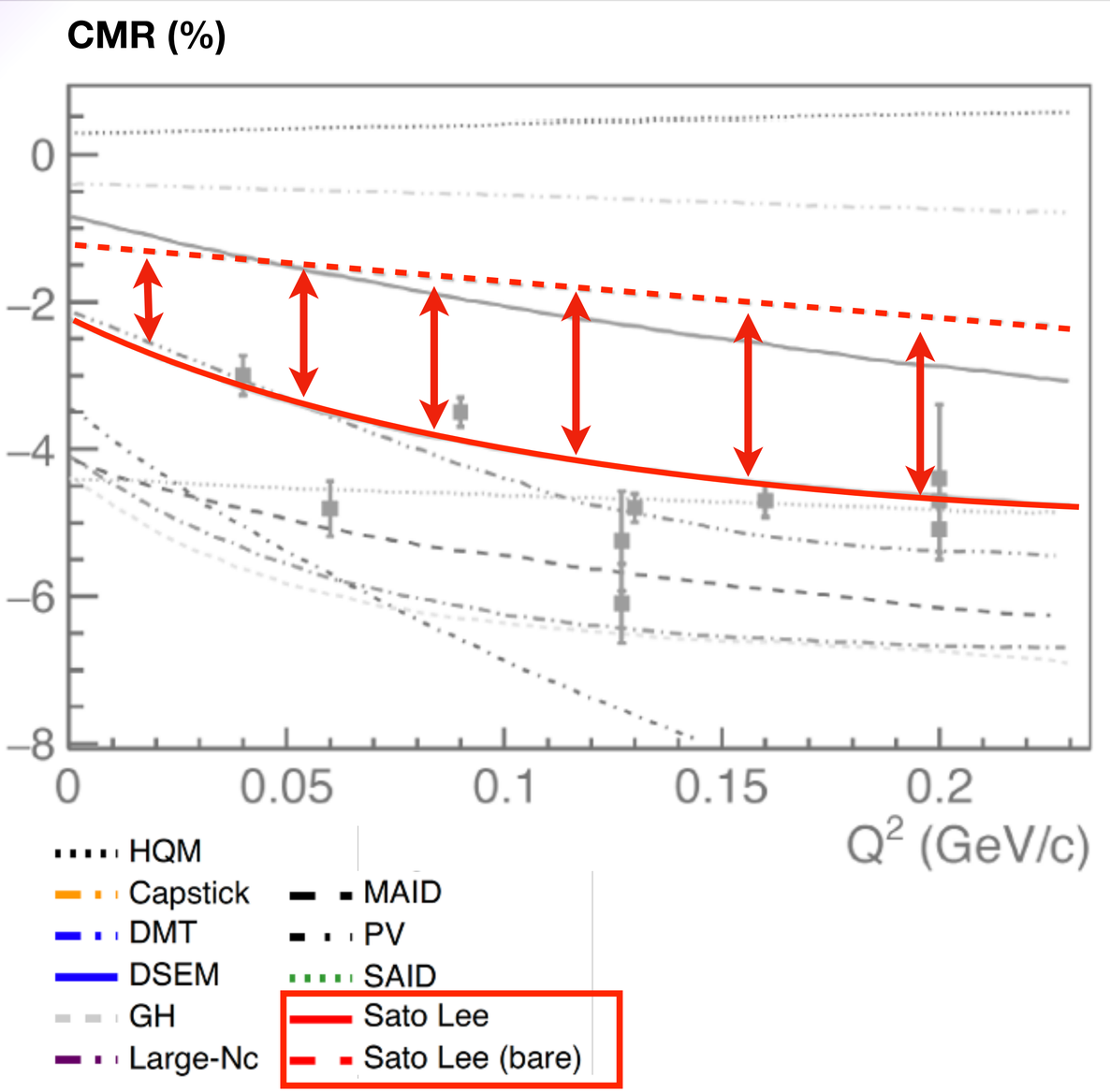

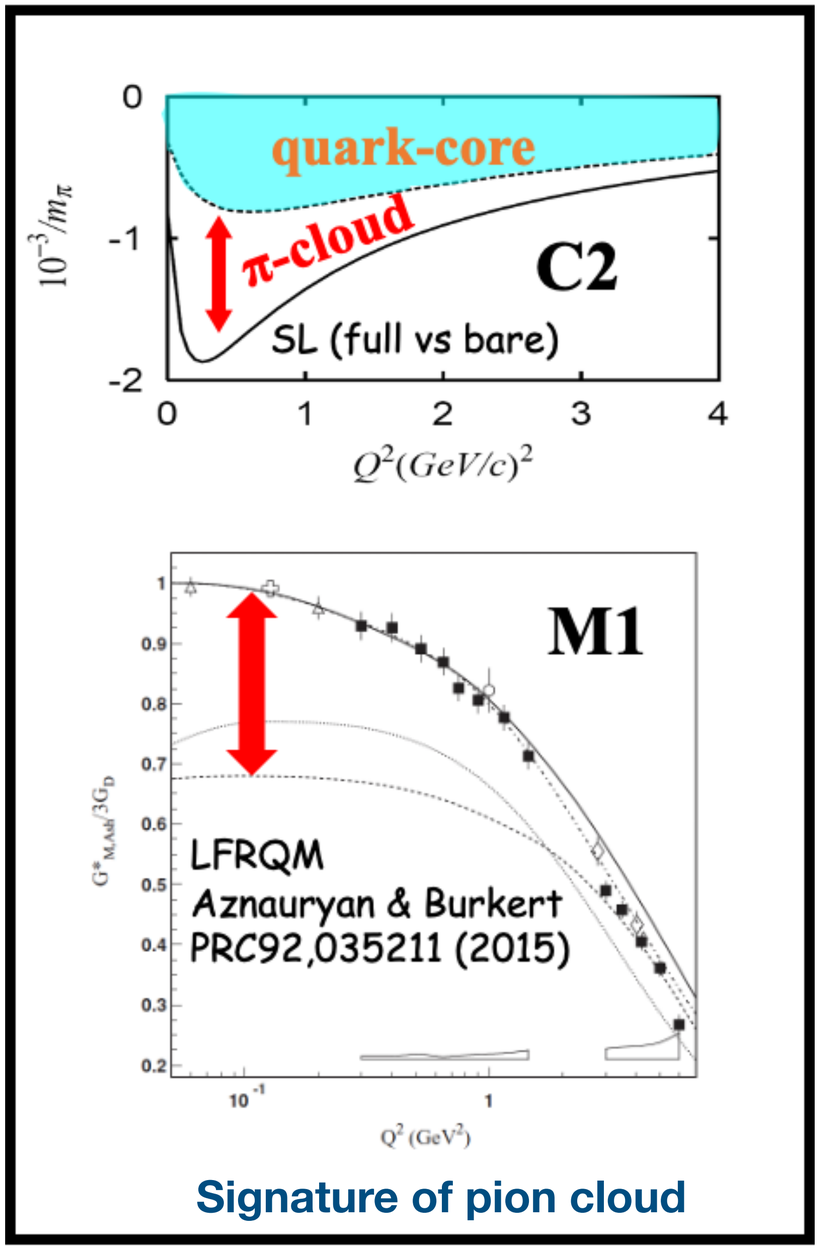

Signature of pion cloud

Dominant role of mesonic d.o.f. at large distance scale:

Mesonic cloud ~ 50% of the quadrupole amplitude magnitude & 1/3 of the magnetic dipole strength

Connections to the neutron structure

- There are long-known relations between the TFFs and the neutron FFs.
  - Pascalutsa, V. & Vanderhaeghen, M. : Phys. Rev. D 76 (2007) [Large-Nc]
  - Grabmayr, P. & Buchmann, A. J. : Phys. Rev. Lett. 86 (2001) [SU(6)]

- G_E^n extraction from TFFs show strong agreement with world data.
  - Allows access to low-Q^2 region where direct measurement of G_E^n is difficult.

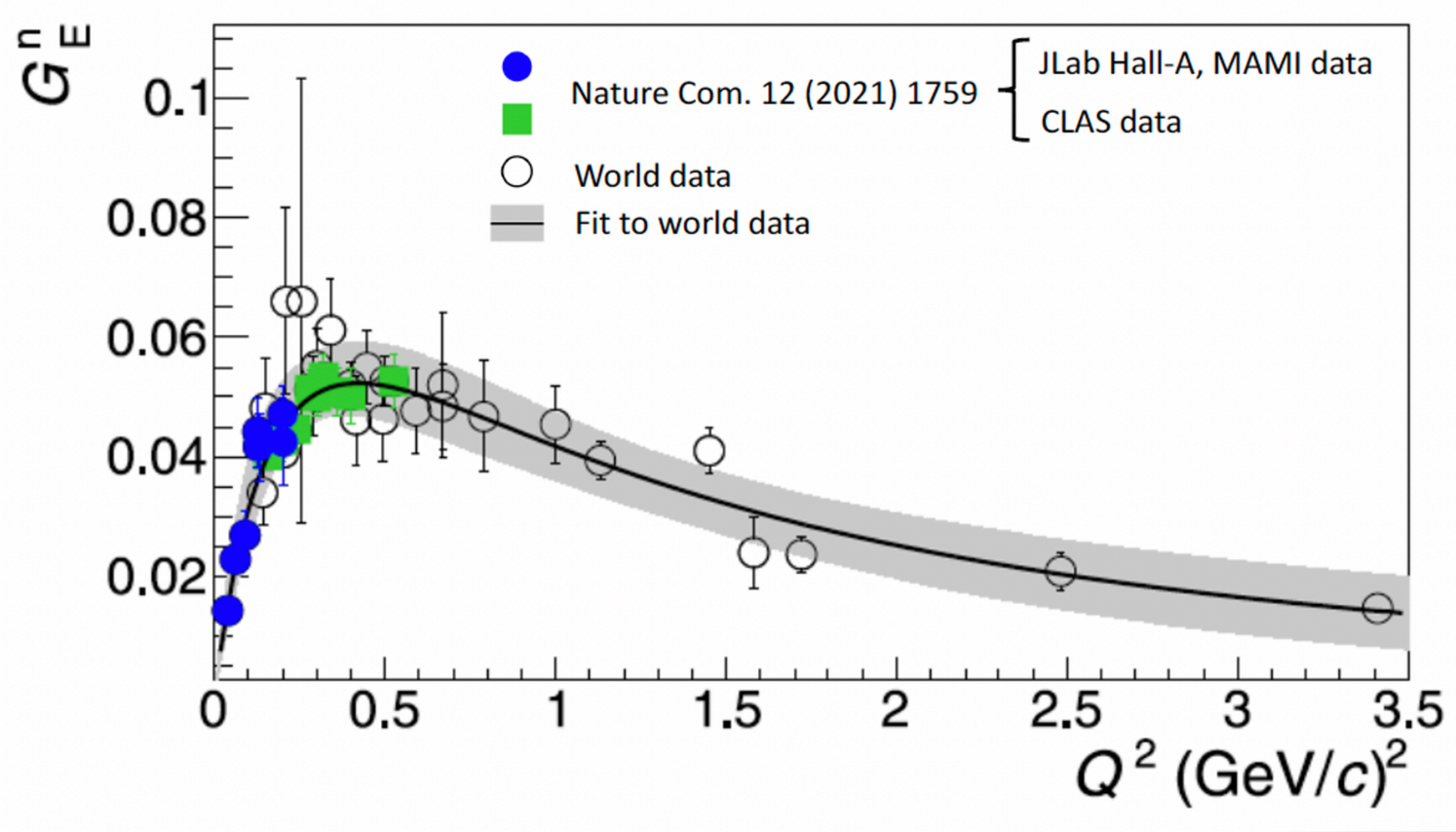

JLab E12-15-001 Experiment

Hall C HMS and SHMS

SHMS:
- 11-GeV Spectrometer
- Partner of existing 6-GeV **HMS**

MAGNETIC OPTICS:
- Point-to Point QQQD for easy calibration and wide acceptance.
- Horizontal bend magnet allows acceptance at forward angles (5.5°)

Detector Package:
- Drift Chambers
- Hodoscopes
- Cerenkovs
- Calorimeter
- All derived from existing HMS/SOS detector designs

Well-Shielded Detector Enclosure

Rigid Support Structure
- Rapid & Remote Rotation
- Provides Pointing Accuracy & Reproducibility demonstrated in HMS

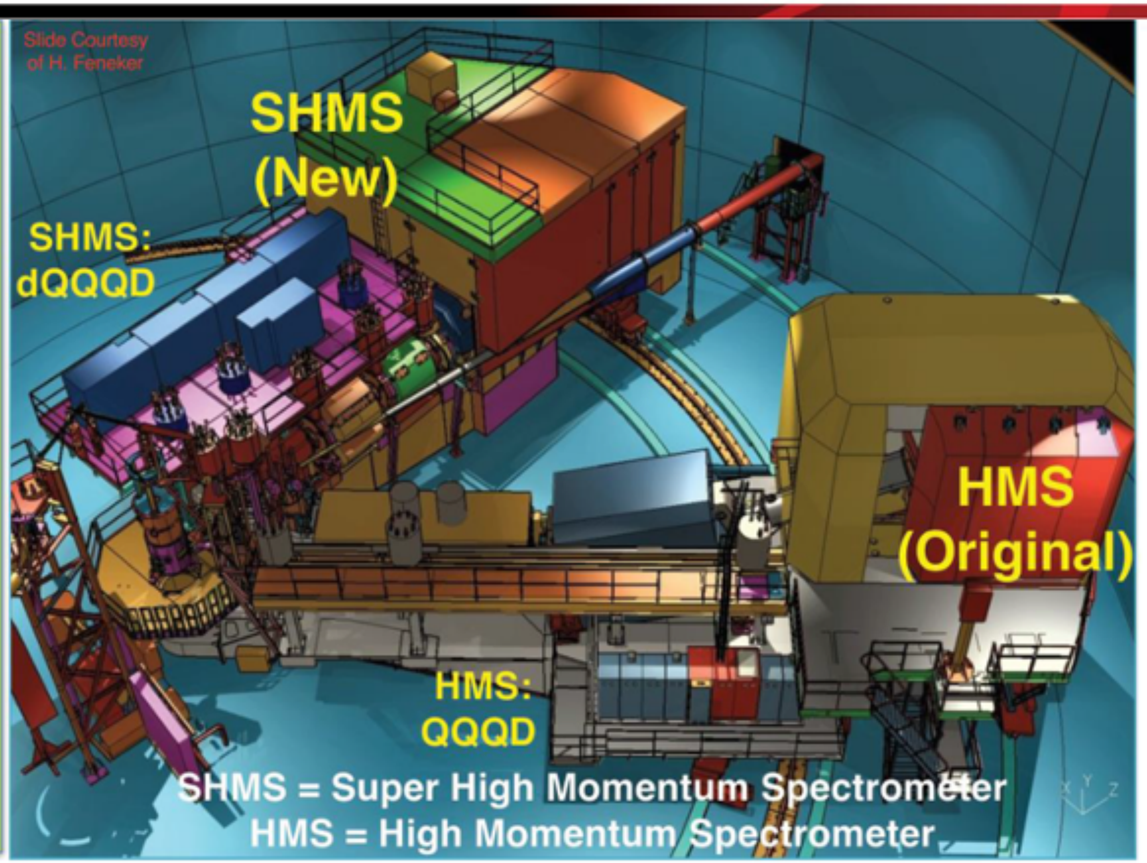

- Summer 2019: July 20 - August 5

JLab E12-15-001 Experiment

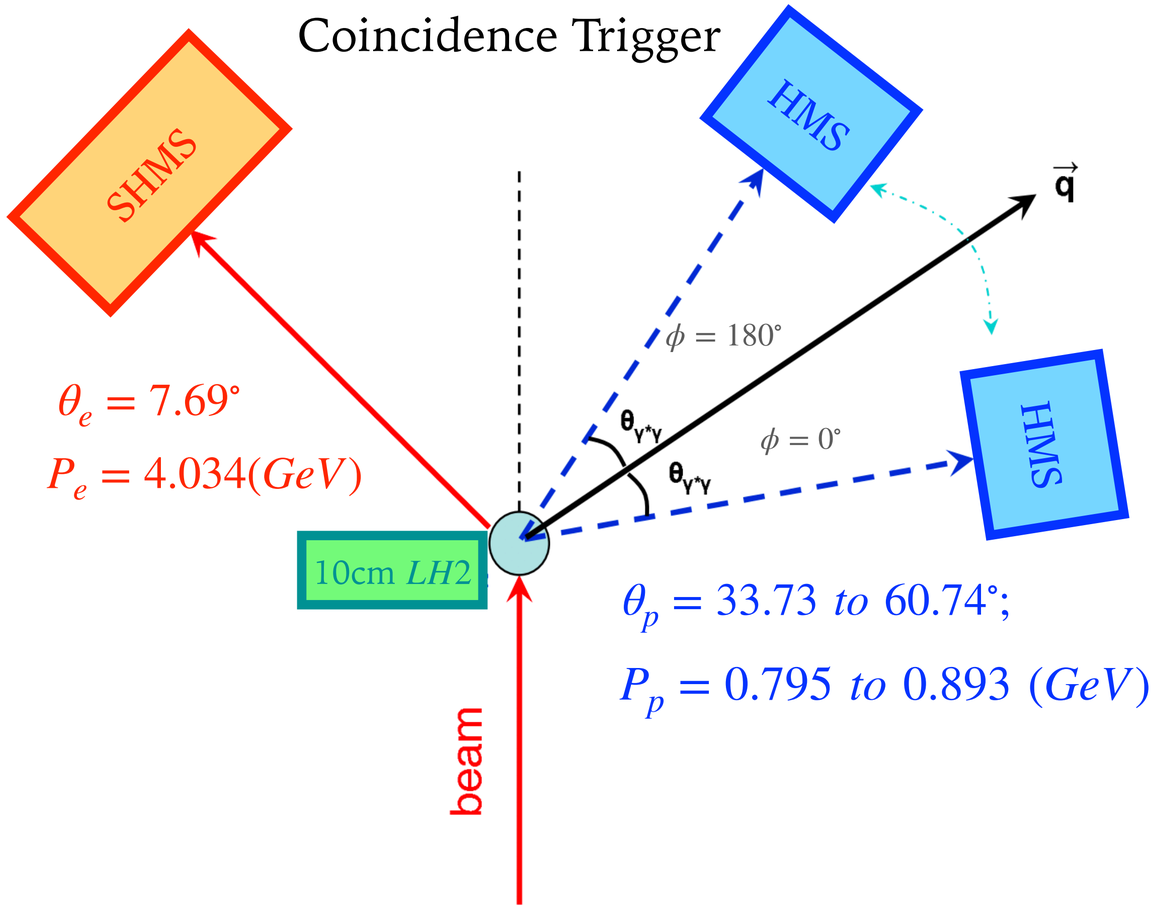

	Kinematical Setting	$\theta_{\gamma^*\gamma}{}^\circ$	$\theta_e{}^\circ$	$P_e'(MeV/c)$	$\theta_p{}^\circ$	$P_p'(MeV/c)$	S/N	beam time (days)
Part I	Kin Ia	155	7.97	3884.4	37.20	893.20	1.1	0.5
	Kin Ib	155	7.97	3884.4	51.26	893.20	2.7	0.5
	Kin IIa	140	7.97	3884.4	33.08	859.90	1	0.45
	Kin IIb	140	7.97	3884.4	55.38	859.90	3.7	0.55
	Kin IIIa	120	7.97	3884.4	27.85	794.68	0.9	0.45
	Kin IIIb	120	7.97	3884.4	60.61	794.68	6.2	0.55
	Kin IVa	165	9.39	3820.5	40.85	1010.40	1.3	0.5
	Kin IVb	165	9.39	3820.5	48.45	1010.40	2.4	0.5
	Kin Va	155	9.39	3820.5	38.34	995.20	1	0.5
	Kin Vb	155	9.39	3820.5	50.96	995.20	3.2	0.5
	Kin VIa	128	9.39	3820.5	31.84	919.43	0.7	0.95
	Kin VIb	128	9.39	3820.5	57.46	919.43	7.8	0.55
Part II	Kin VIIa	165	11.54	3708.6	40.81	1175.25	2.6	1.5
	Kin VIIb	165	11.54	3708.6	47.35	1175.25	5	2
	Kin VIIIa	160	11.54	3708.6	39.73	1167.72	2.2	1.5
	Kin VIIIb	160	11.54	3708.6	48.43	1167.72	6.3	2
	Kin IXa	140	11.54	3708.6	35.52	1117.38	1.2	1.5
	Kin IXb	140	11.54	3708.6	52.64	1117.38	8	2

Part I

Part II

- Summer 2019: July 20 - August 5
- Beam $E = 4.56GeV$
- $Q^2 = 0.25 - 0.4\ GeV^2$, $W = 1.232\ GeV$

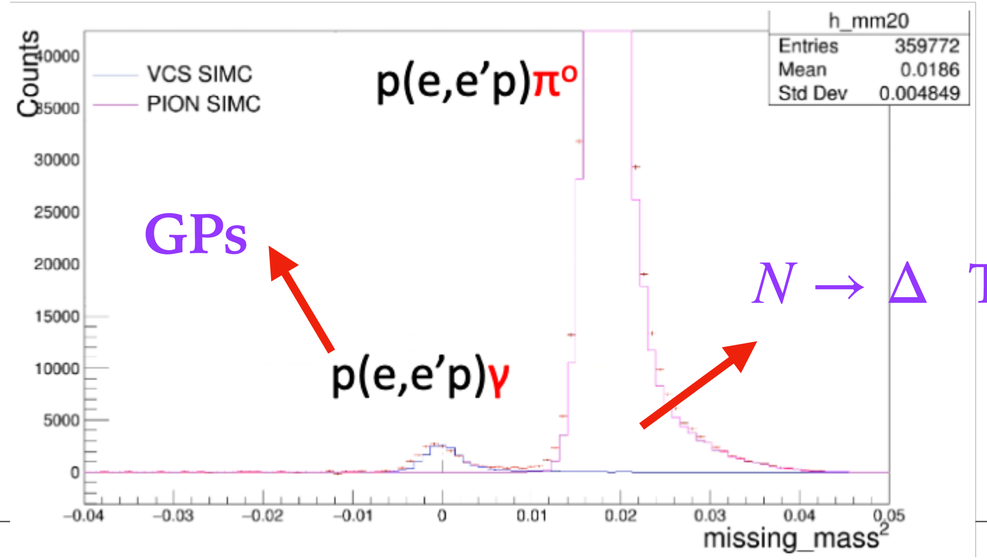

Elastic Data

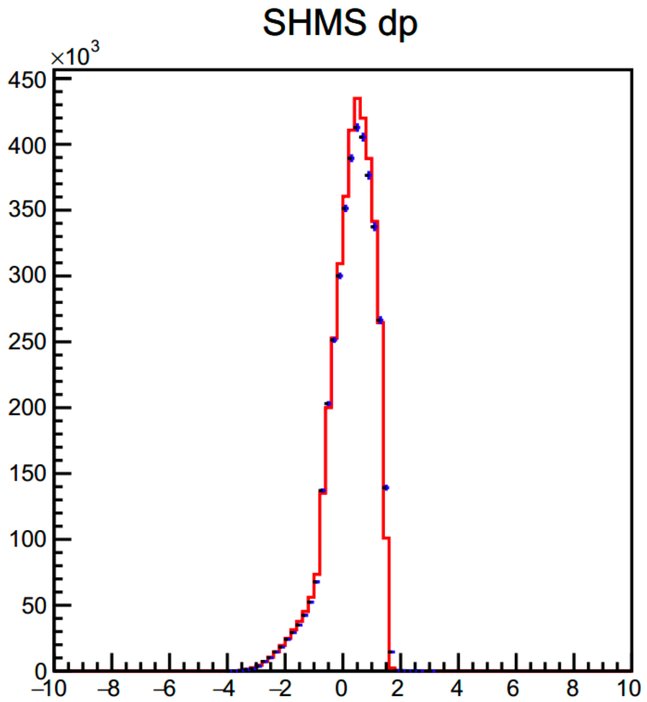

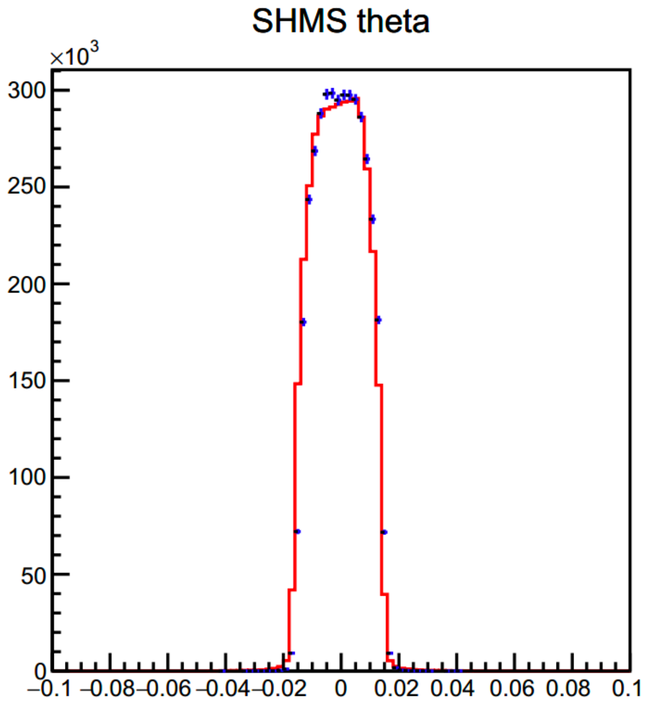

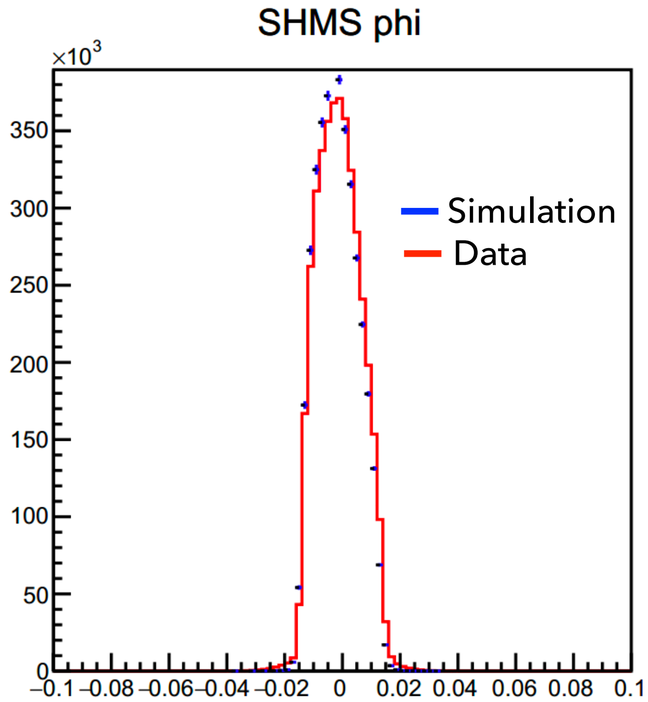

Kinematic	θ_e°	$P_e(GeV/c)$	θ_p°	$P_p(GeV/c)$
Elastic I	10.76	4.193	61.16	0.893
Elastic II	10.41	4.214	61.95	0.863
Elastic III	9.64	4.259	63.76	0.795

π^0 Analysis

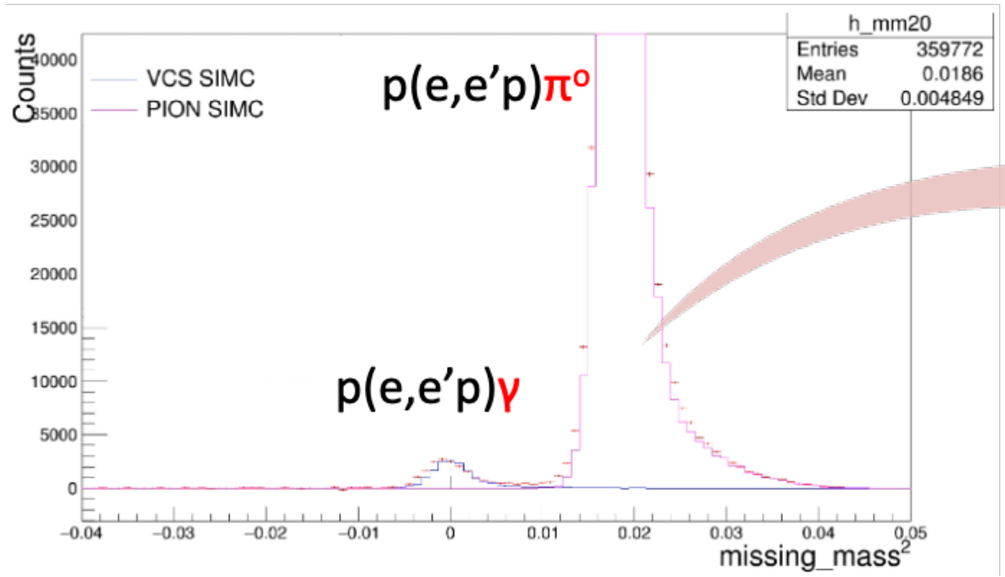

W

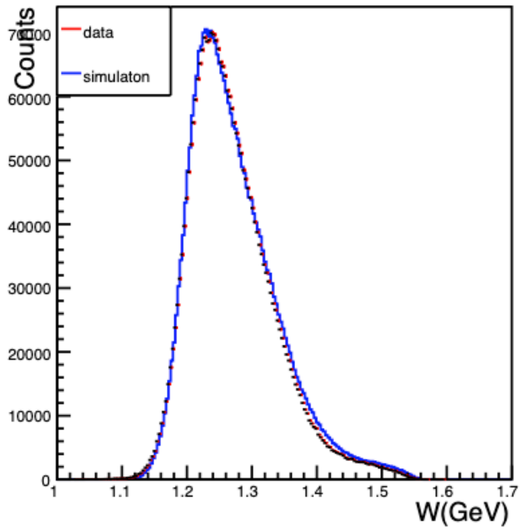

MAID
Data

θ_{pq}

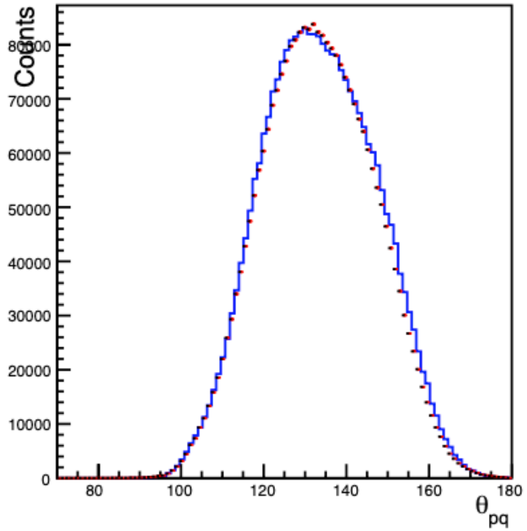

π^0 Cross Sections

- Q^2=0.36 (GeV/c)^2

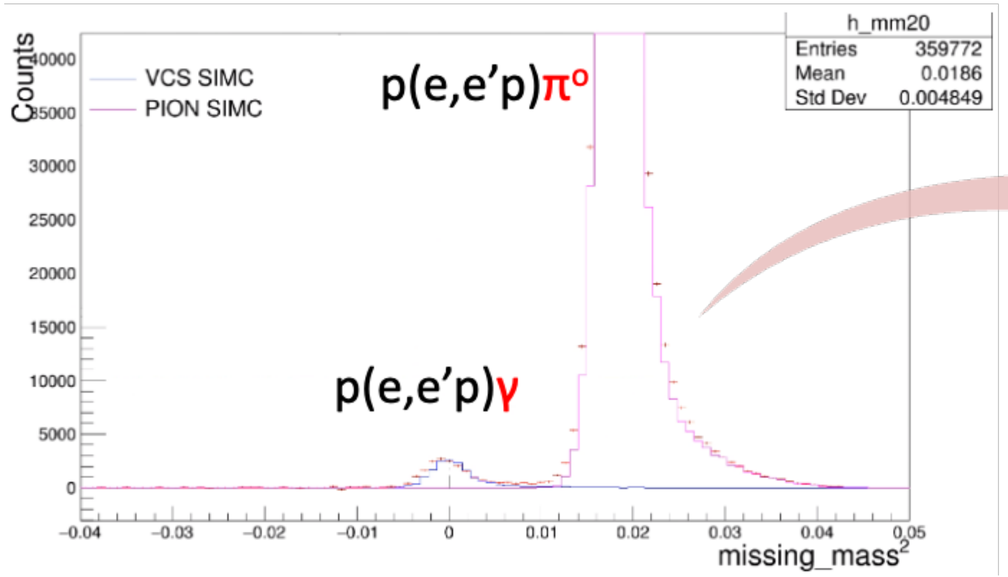

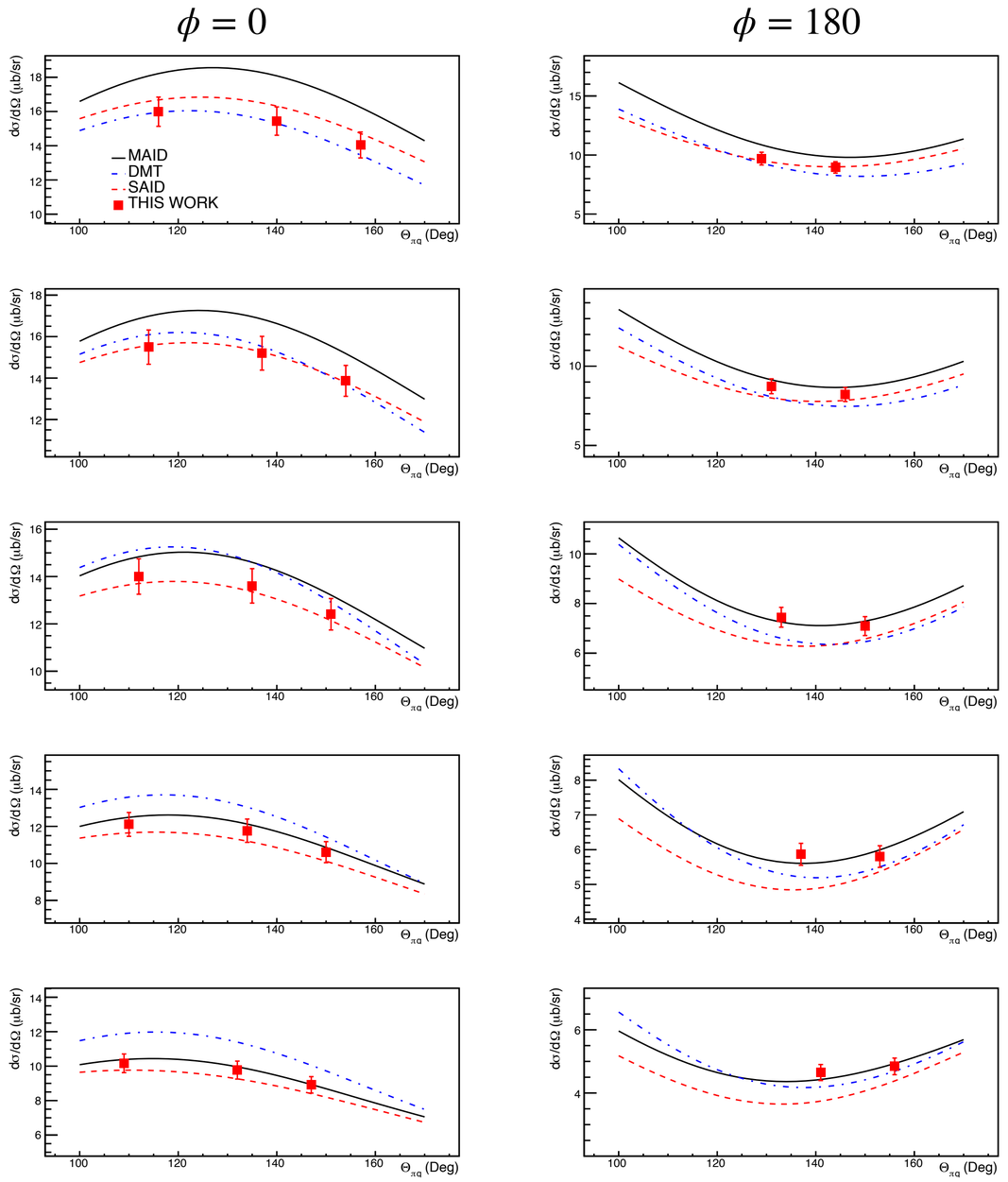

π^0 Cross Sections

- Q^2=0.36 (GeV/c)^2

In Plane

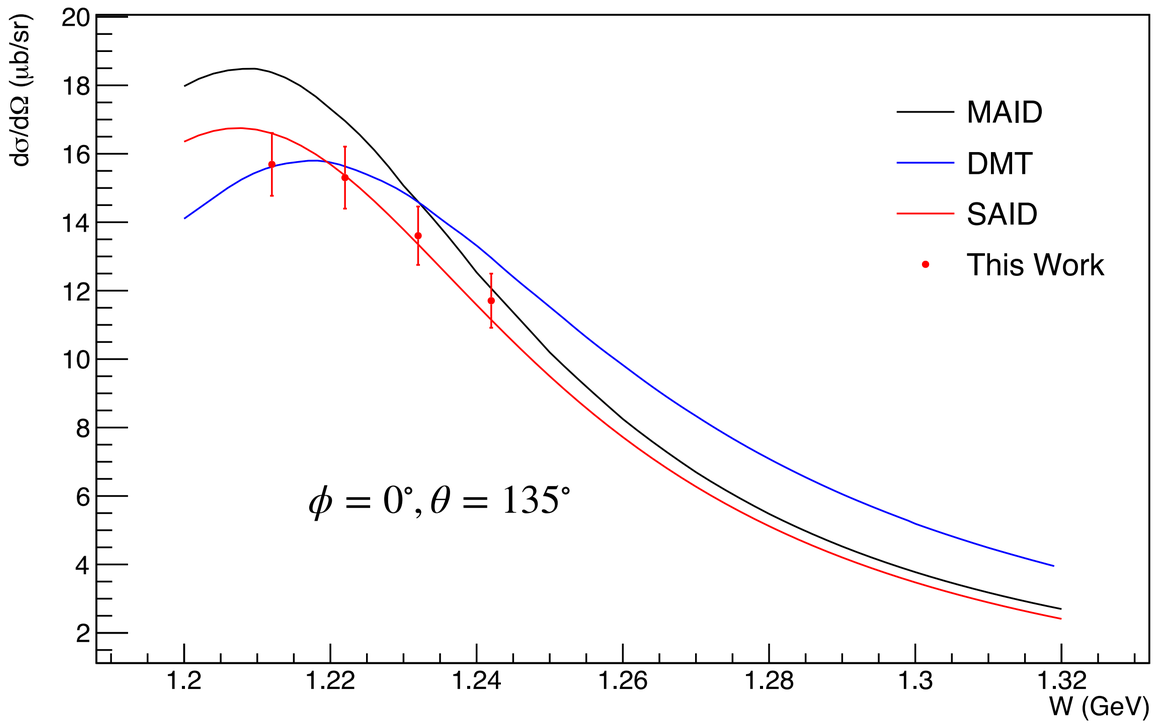

Out of Plane

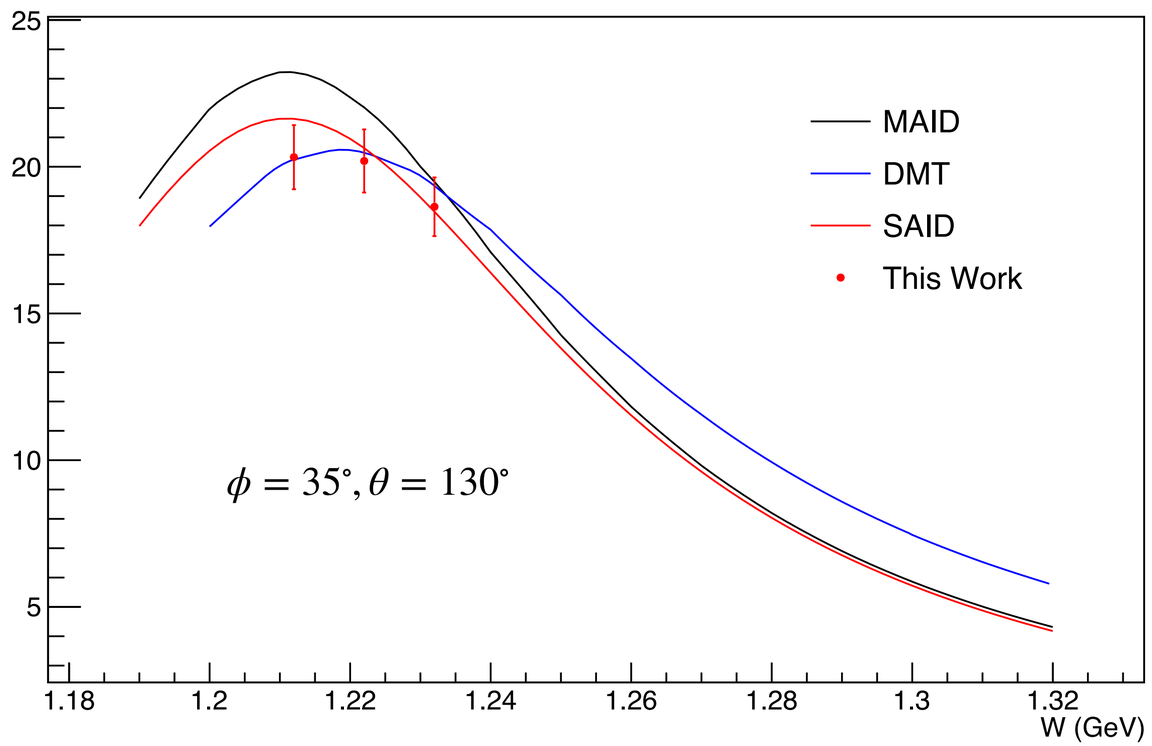

$N \rightarrow \Delta$ Transition Form Factors

M1 - Magnetic dipole amplitude
C2 - Coulomb quadrupole amplitude
E2 - Electric quadrupole amplitude

CMR = C2/M1
EMR = E2/M1

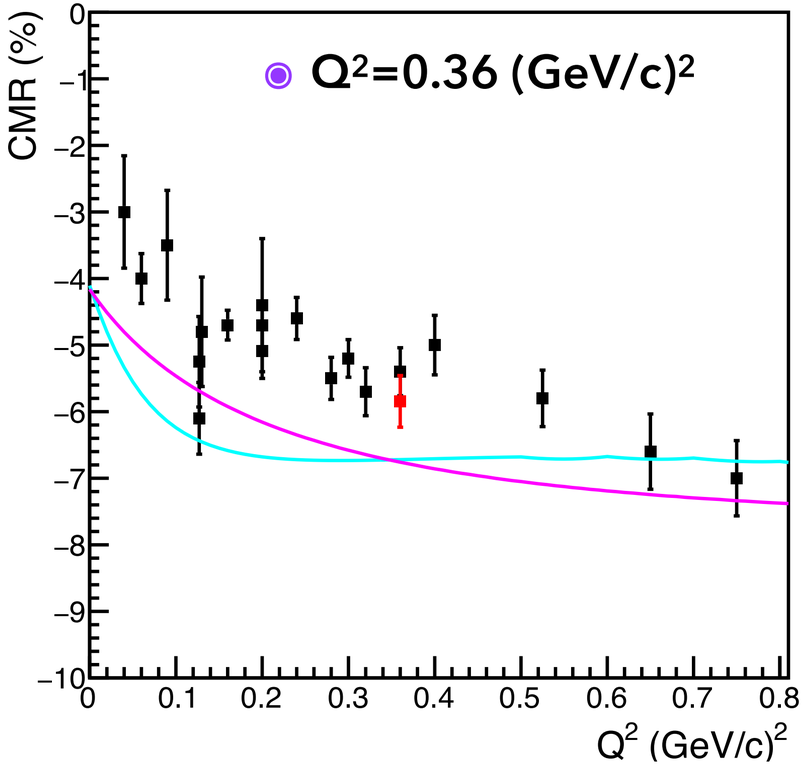

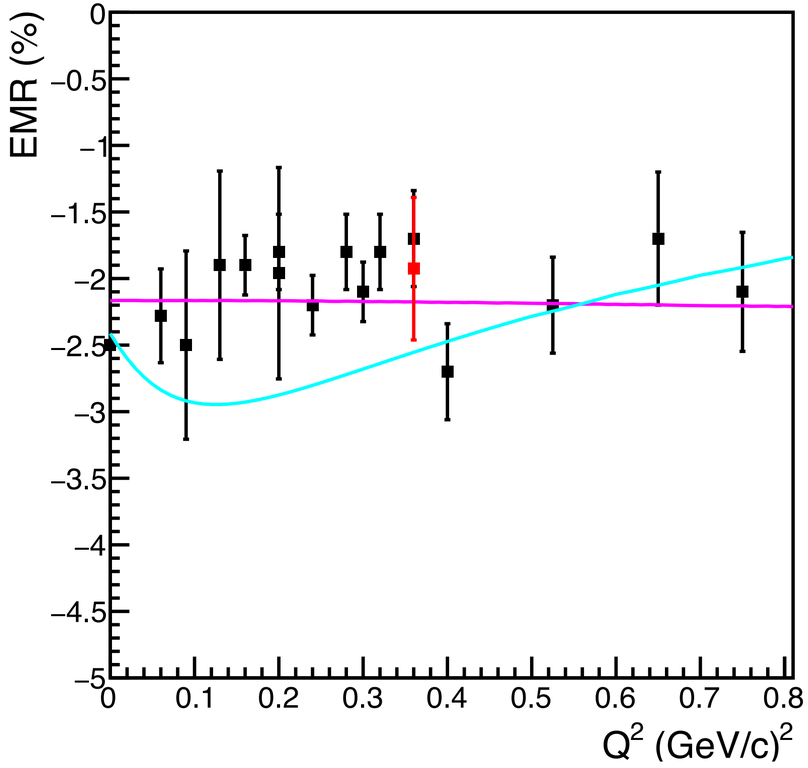

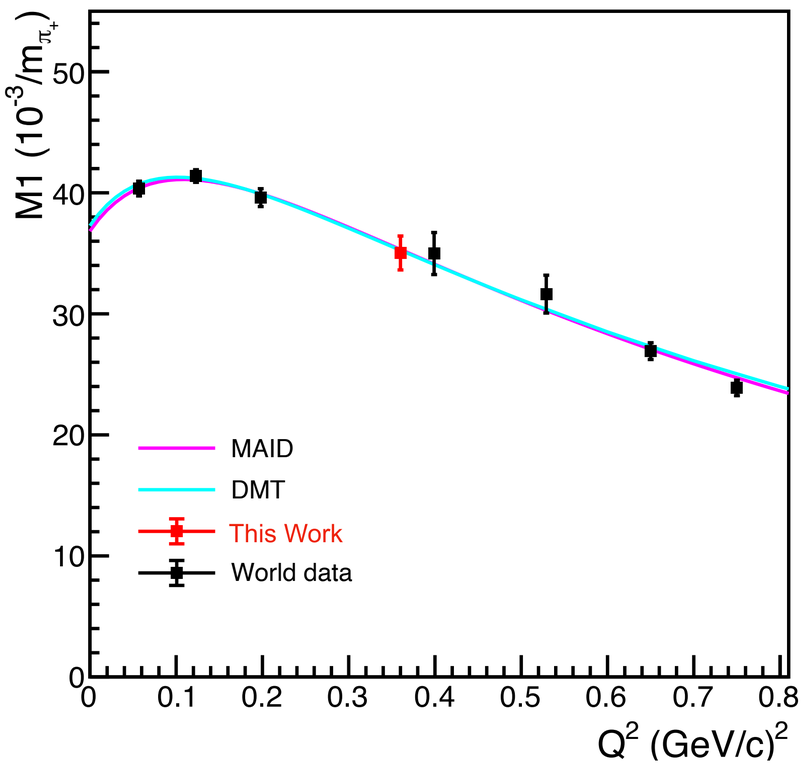

New Experiment

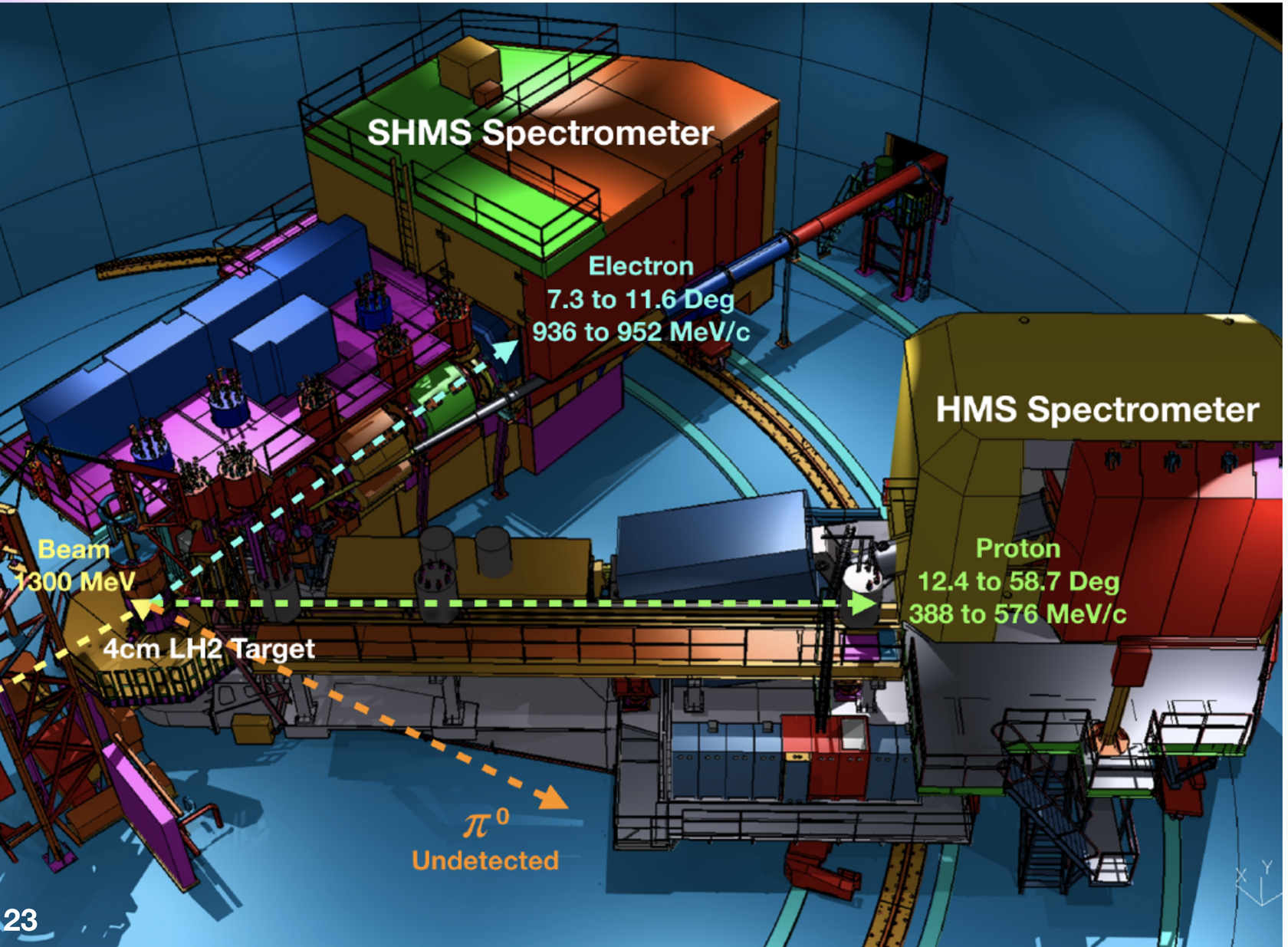

- **Standard Hall-C equipment**
  - 1300 MeV electron beam
  - Detect proton and electron in coincidence
  - Reconstruct pion from missing mass.

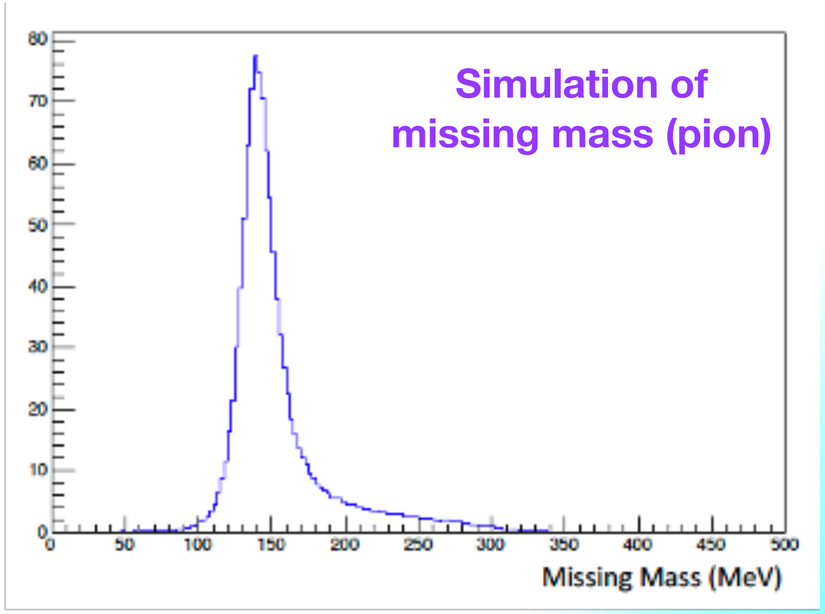

Measurement Settings

Setting	SHMS θ (deg)	SHMS P (MeV/c)	HMS θ (deg)	HMS P (MeV/c)	S/N	Time (hrs)
1a			18.77	532.53	2	7
2a			25.17	527.72	2	7
3a			33.7	506.61	3.2	6
4a	7.29	952.26	42.15	469.66	4.3	5
5a			50.44	418.56	4.9	5
6a			54.47	388.38	4.9	5
7a			12.37	527.72	2.7	6
1b			22.01	547.54	1.2	6
2b			28.24	542.61	1.4	6
3b			36.52	520.95	2.5	5
4b	8.95	946.93	44.64	483.08	3.4	4
5b			52.68	430.78	3.7	4
6b			56.53	399.92	3.5	4
7b			12.46	535.98	1.6	5
1c			24.40	562.00	1.5	9
2c			30.47	556.95	1.9	9
3c			38.52	534.79	3.5	6
4c	10.37	941.61	46.47	496.06	4.4	6
5c			54.17	442.64	4.8	6
6c			57.85	411.16	4.8	6
7c			12.69	543.24	2	6
1d			26.24	575.96	1.8	12
2d			32.16	570.80	2.5	11
3d			40.01	548.17	4.5	8
4d	11.63	936.28	47.73	508.64	5.5	8
5d			55.18	454.17	6.9	7
6d			58.71	422.13	6	8
7d			12.47	548.17	2.1	10

- **Cover a Q^2 range of 0.015 to 0.055 $(GeV/c)^2$**
  - 28 arm configurations
  - Coverage for 9 Q^2 bins.
  - 8 days production
  - 3 days other (dummy, calibration, etc..)

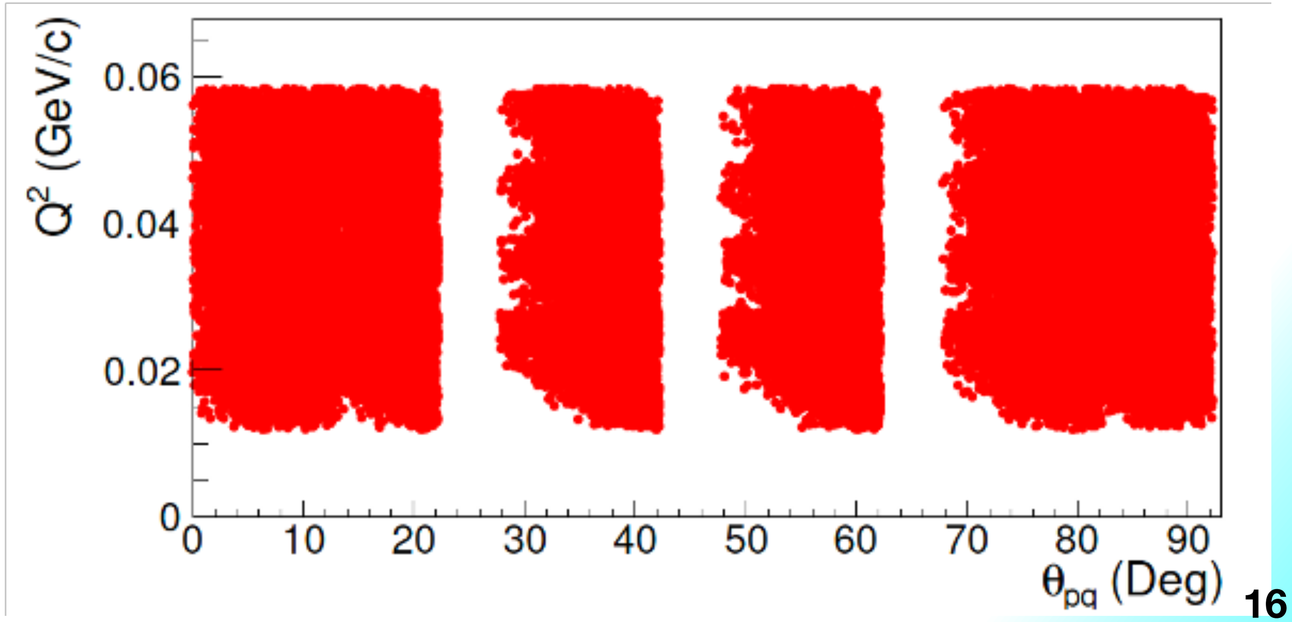

Projected CMR and EMR measurements

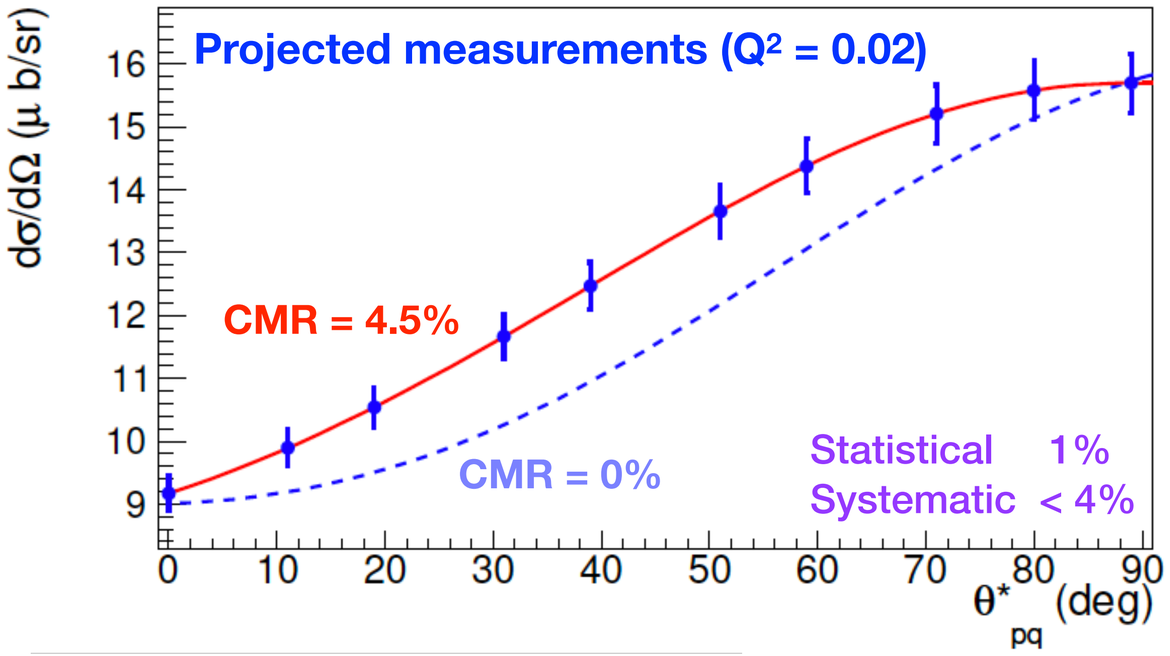

Resolution	2% - 3%
Acceptance	1%
Scattering angle	0.4% - 0.6%
Beam energy	0.7% - 1.2%
Beam charge	1%
Target density	0.5%
Detector efficiencies	0.5%
Target cell background	0.5%
Target length	0.5%
Dead-time corrections	0.5%
Total	2.8% - 3.8%

- High precision in very low Q^2 region that is sparsely populated
  - Region where pion-cloud effects are expected to be prominent

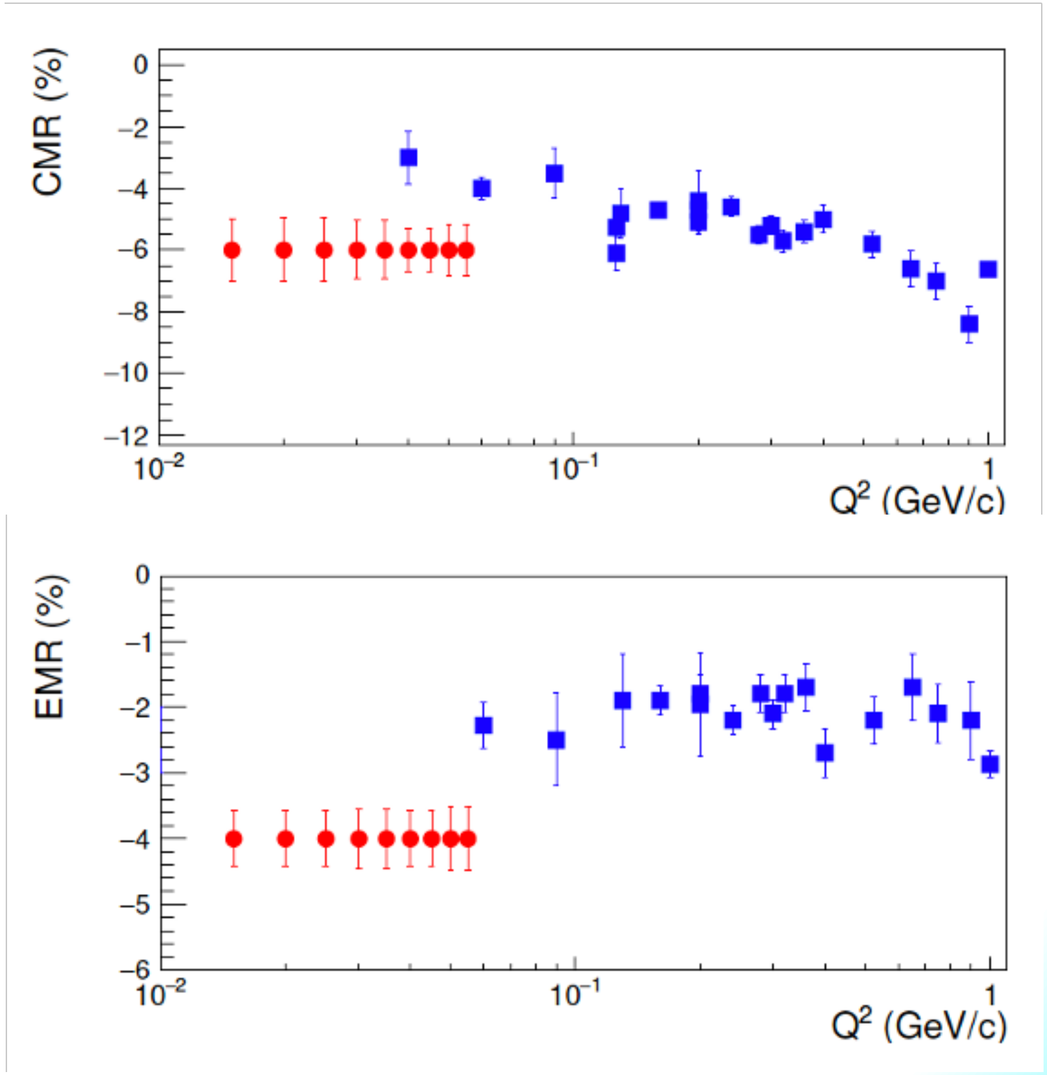

Projected CMR and EMR measurements

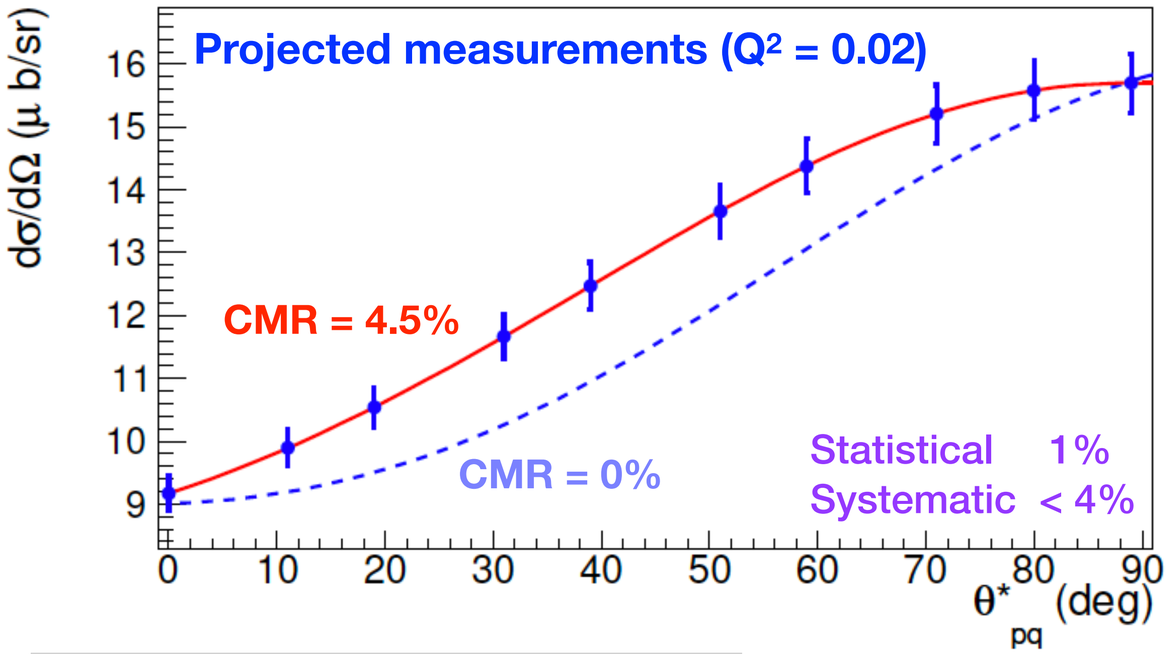

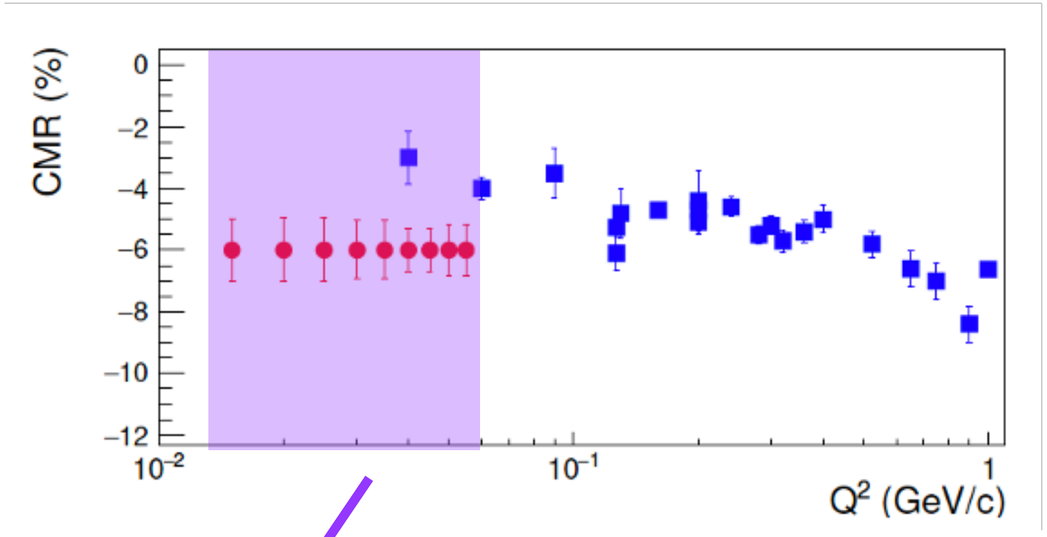

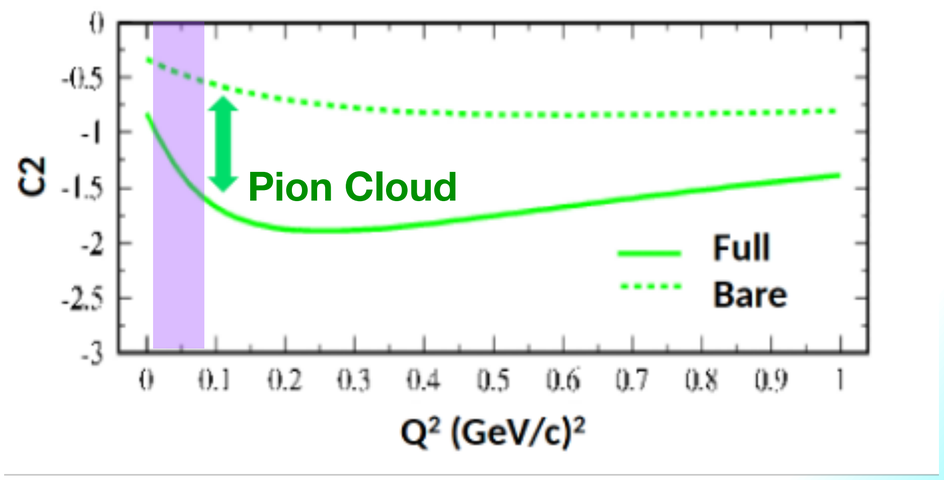

Resolution	2% - 3%
Acceptance	1%
Scattering angle	0.4% - 0.6%
Beam energy	0.7% - 1.2%
Beam charge	1%
Target density	0.5%
Detector efficiencies	0.5%
Target cell background	0.5%
Target length	0.5%
Dead-time corrections	0.5%
Total	2.8% - 3.8%

- High precision in very low Q^2 region that is sparsely populated
  - Region where pion-cloud effects are expected to be prominent

Summary

- **The N→Δ TFFs represent a central element of the nucleon dynamics & has been an important part of Jefferson Lab's experimental program (Halls A, B & C)**
- **CMR, EMR and M1 results were extracted from E12-15-001 Experiment at Q^2=0.36 (GeV/c)^2**
  - High precision measurements in a region that was only accessed by CLAS
  - EMR and CMR results of CLAS are confirmed
  - Adds strong constraints to the theoretical models
  - Publication in process
- **We will extend these measurements in the low Q^2 region:**
  - Test bed for ChEFT calculations
  - High precision benchmark data for the Lattice QCD calculations
  - New constraints and input to the theoretical models
  - Insight to the mesonic-cloud dynamics within a region where they are dominant and rapidly changing
  - Will test if the QCD prediction that CMR & EMR converge as $Q^2 \rightarrow 0$
- **Experiment was approved with A- rating by PAC50**
  - 11 days (8 production, 3 calibration)
  - Beam energy: 1.3 GeV (flexible within +/- 0.1 GeV)
  - Hall C standard SHMS and HMS setup with a 4 cm LH2 target

People

Zulkaida Akbar, Hamza Atac, Vladimir Berdnikov, Deepak Bhetuwal, Debaditya Biswas, Marie Boer, Alexandre Camsonne, Jian-Ping Chen, Eric Christy, Arthur Conover, Markus Diefenthaler, Burcu Duran, Dipangkar Dutta, Rolf Ent, Dave Gaskell, Carlos Ayerbe Gayoso, Ole Hansen,Florian Hauenstein, Nathan Heinrich, William Henry, Tanja Horn, Joshua Hoskins, Garth Huber, Shuo Jia, Mark Jones, Sylvester Joosten, Abishek Karki, Stephen Kay, Vijay Kumar, Ruonan Li, Xiaqing Li, Wenliang Li,Anusha Habarakada Liyanage, Dave Mack, Simona Malace, Pete Markowitz, Mike McCaughan, Hamlet Mkrtchyan, Casey Morean, Mireille Muhoza, Amrendra Narayan, Michael Paolone, Melanie Rehfuss, Brad Sawatzky, Andrew Smith, Greg Smith, Nikolaos Sparveris, Richard Trotta, Carlos Yero, Xiaochao Zheng, Jingyi Zhou

Spokespersons Run Coordinators Research Faculty Graduate student

Thank You !

Hamza Atac
Temple University

Supported by the US DOE / NP award DE-SC0016577

On behalf of JLAB E12-15-001 Collaboration

Jefferson Lab

U.S. DEPARTMENT OF ENERGY